

Simulation of ion-scale solar wind turbulence using extended fluid modeling

Thierry Passot

UCA, CNRS, Observatoire de la Côte d'Azur, Nice, France

Collaborators:

D. Borgogno, P. Henri, P. Hunana, D. Laveder and P.L. Sulem

Advances in geophysical and astrophysical turbulence

Cargèse, France

25 July -5 August 2016

Outline

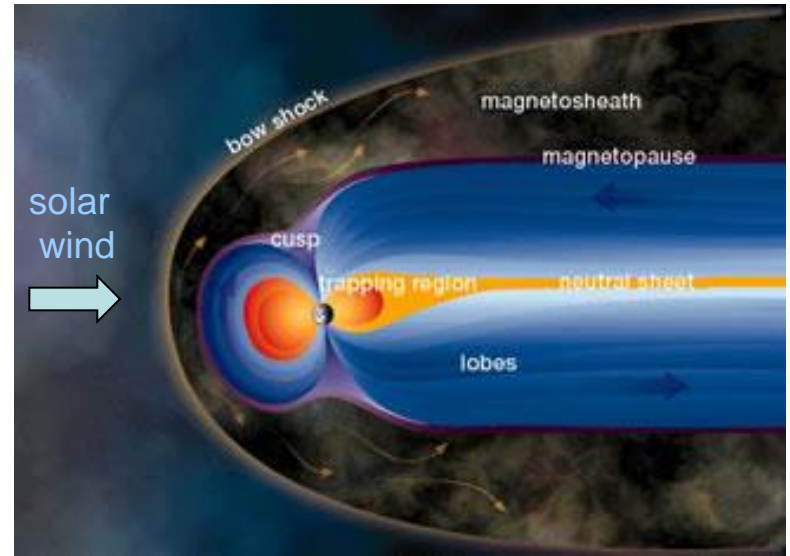
- The meso-scale solar wind context:
 - Importance of compressibility, dispersion, dissipation
- Fluid approaches: from incompressible MHD to the Landau fluid model
- The FLR Landau fluid model:
 - properties of the linear system and consistency with gyrofluids in the limits of large and small transverse scales in the weakly nonlinear case
- 3D simulations of (kinetic) Alfvén wave turbulence
- Non-universal properties of the sub-ion range magnetic energy spectrum
- Conclusions

Main features of 1 AU solar wind plasmas

Space plasmas are magnetized and turbulent with essentially no collision.

β (ratio of thermal to magnetic pressures) $\approx .1\text{--}10$
 M_s (ratio of typical velocity fluctuations to sonic velocity) $\approx 0.05\text{ -- }0.2$

Fluctuations: power-law spectra extend to ion gyroscale and below



Dispersive and kinetic effects cannot be ignored.

Presence of coherent structures (filaments, shocklets, magnetosonic solitons, magnetic holes) with typical scales of a few ion Larmor radii.

The concepts of waves make sense even in the strong turbulence regime

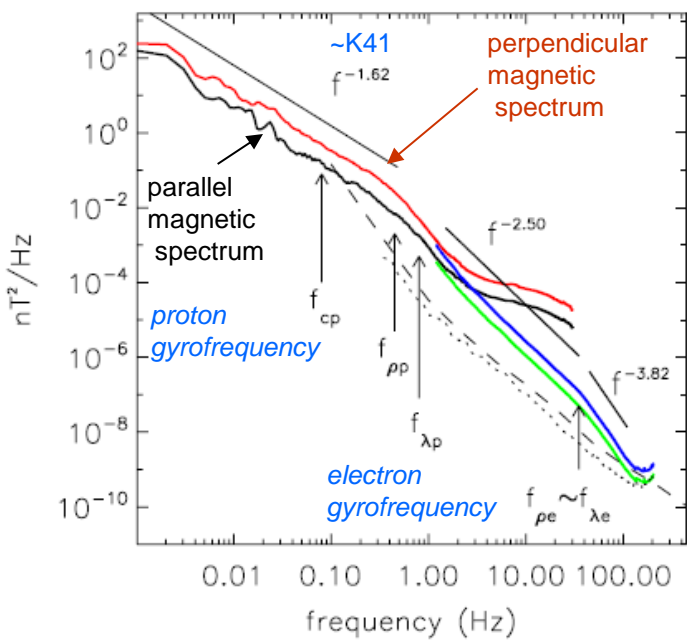
For reviews see e.g. :

Alexandrova et al. *SSR*, **178**, 101 (2013);
Bruno & Carbone, *Liv. Rev. Solar Phys.* **10**, 2 (2013).

Debated questions

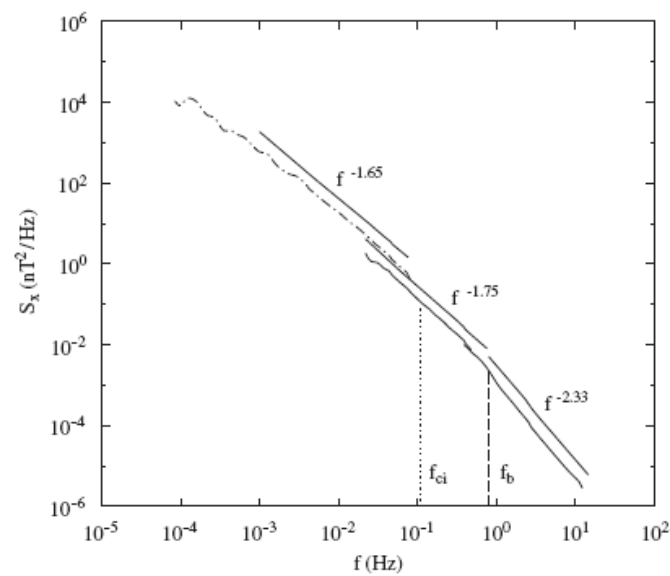
1. Spectral energy distribution and its anisotropy in the solar wind

Several power-law ranges: Are they cascades? strong or wave turbulence? which waves? which slopes? Important to estimate the heating rates.



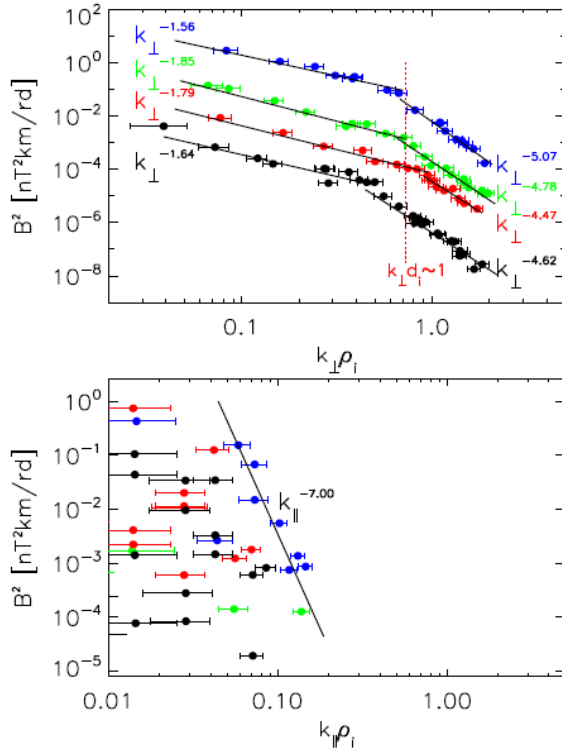
Sahraoui et al. PRL 102, 231102 (2009)

k-filtering $\rightarrow \theta=86^\circ$

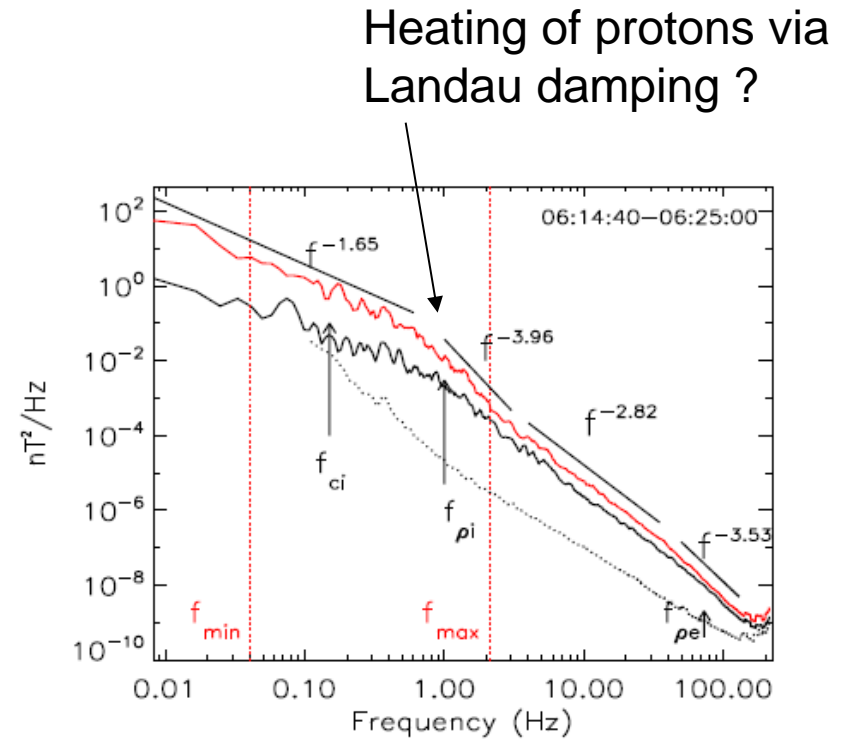


Alexandrova et al. Planet. Space Sci. 55, 2224 (2007)

Does the anisotropy persist at small scales?



At what scale(s) does dissipation take place? By which mechanism?
Role of ion and electron Landau damping ?



From Sahraoui et al. PRL (2010).

2. Main features of magnetosheath plasma

Important role of the temperature anisotropy:

AIC (near quasi-perpendicular shock) and mirror instabilities (further inside magnetosheath)

Very strong compressibility.

Many cases with k^{-1} spectrum at large scales (or even shallower, see e.g. Hadid et al. ApJL 813, L29, 2015 for the Kronian case)

Presence of :

- mirror modes

Here identified as mirror modes using k-filtering technique,

(Pinçon & Lefèuvre, JGR 96, 1789; 1991):

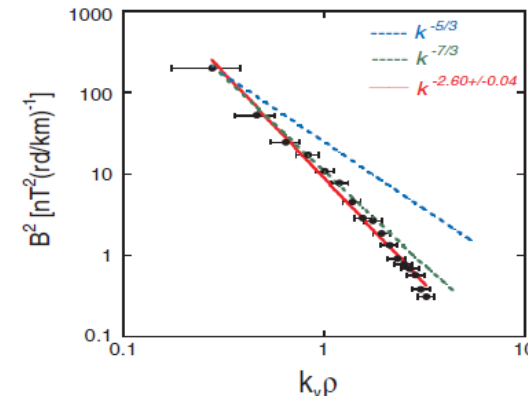
these modes have essentially zero frequency in the plasma frame

- slow waves

- coherent structures:

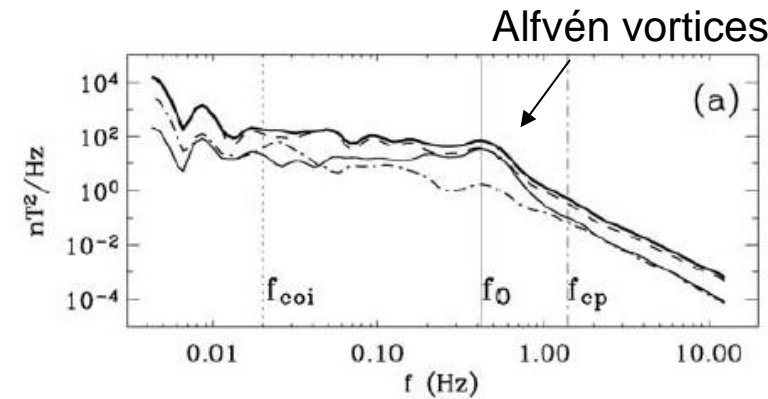
- Current filaments

- Mirror structures (magnetic holes and humps)



spatial spectrum steeper
than temporal one

Sahraoui et al. PRL 2006



Alexandrova et al. JGR 111, A12208 (2006).

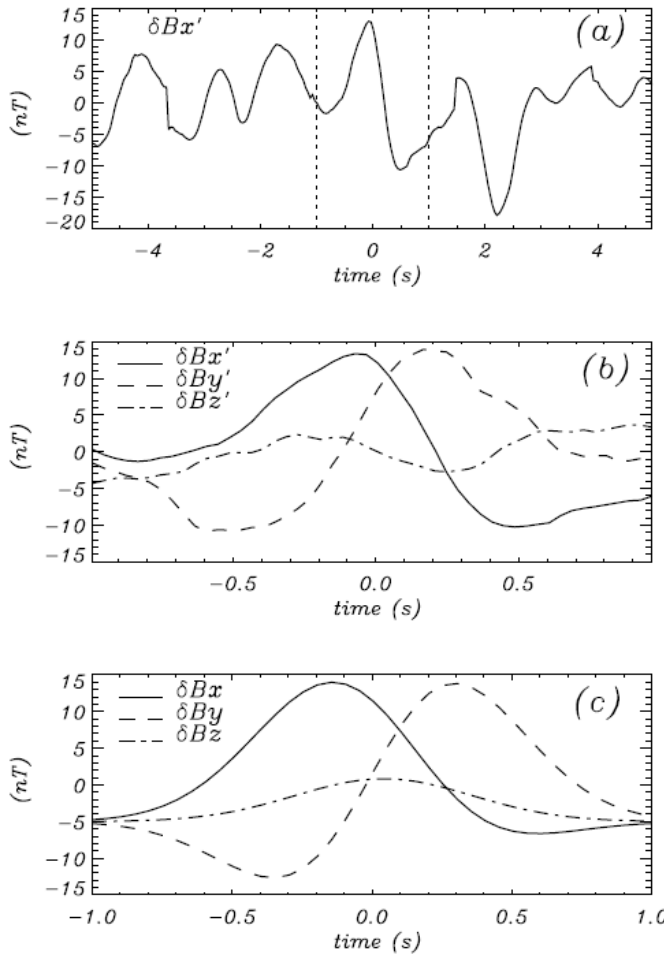


Figure 8. Magnetic field fluctuations, taking $\tau \simeq -420$ s (1755:16 UT) as the origin of time. (a) Fluctuations $\delta B_x'$ during 10 s around τ . (b) Fluctuations of the magnetic field components ($\delta B_x'$, $\delta B_y'$, $\delta B_z'$) for the 2-s period around τ . (c) The z -aligned current tube simulation (δB_x , δB_y , δB_z).

Signature of magnetic filaments
(Alexandrova et al. JGR 2004)

Also « compressible vortices »
(Perrone et al. ApJ 2016, in press)

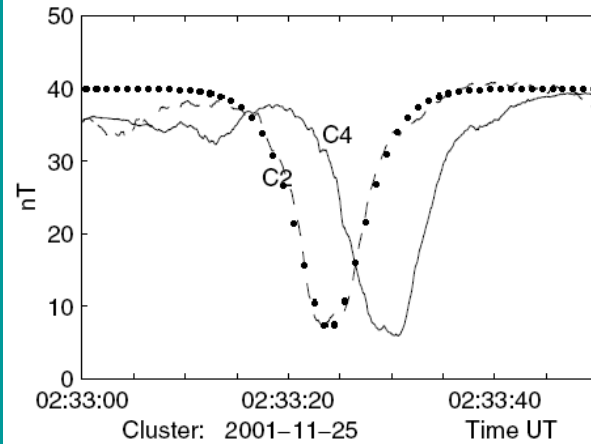
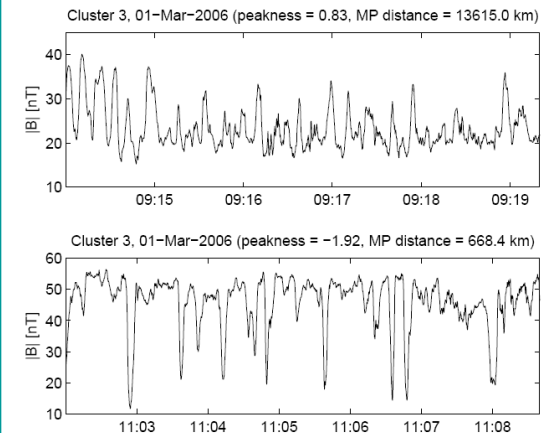
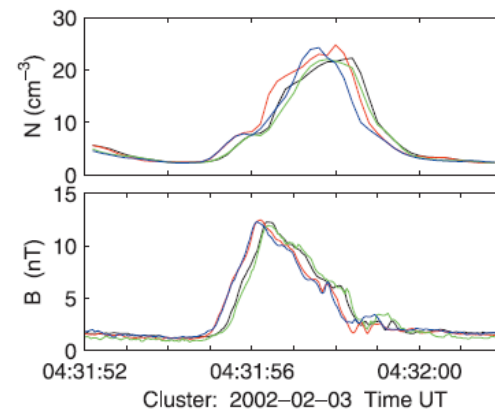


FIG. 1. A large scale soliton observed by Cluster spacecraft C2 (dashed) and C4 (solid) in the total magnetic field. Marked curve shows fit of $b_0 \operatorname{sech}^2[(t - t_0)/\delta t]$ with $b_0 = -33$ nT and $\delta t = 4.4$ s. The soliton moves with velocity $u_0 \approx 250$ km/s and has a width of 2000 km. The position of Cluster satellites was $(-4, 17, 5) R_E$ GSE.

Slow magnetosonic solitons
(Stasiewicz et al. PRL 2003)



Mirror structures in the terrestrial magnetosheath
(Soucek et al. JGR 2008)

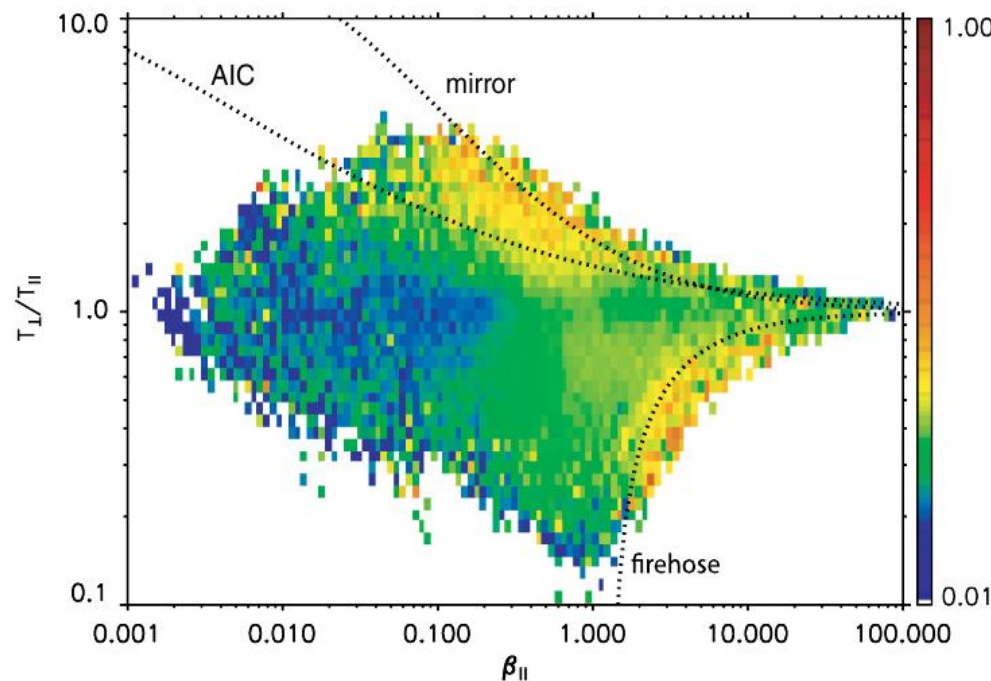


Fast magnetosonic shocklets
(Stasiewicz et al. GRL 2003)

Figure 2. Pulse-like enhancements of the plasma density and magnetic field measured on four Cluster spacecraft: C1–C4, which are color coded in sequence: black, red, green, blue. The measurements represent signatures of fast magnetosonic shocklets moving with supersonic speed in a high- β plasma.

2. Heating of the plasma: temperature anisotropy and resulting micro-instabilities

Turbulence (and/or solar wind expansion) generate **temparature anisotropy**
This anisotropy is limited mostly by **mirror and oblique firehose** instabilities.
Role of anisotropy on the turbulence « dissipative range»?



*Bale et al. PRL 103, 21101 (2009);
see also Hellinger et al. GRL 33, L09101 (2006).*

color: magnitude of δB ; enhanced δB also corresponds
to enhanced proton heating.

As a summary, the **solar wind at meso-scales¹** has the following main characteristics:

- very few collisions
- moderately strong guide field
- non-negligible compressibility
- decoupling between ion and electron velocities
- anisotropic pressures
- dissipative effects such as Landau damping at several scales
- co-existence of strong turbulent structures and waves

¹: i.e. at scales close to the ion gyroradius.

In view of the difficulty in performing numerical simulations of the full Vlasov equation (or even its hybrid and/or **gyrokinetic²** reductions), it is desirable to look for appropriate fluid models.

² kinetic equation with averaging over particles Larmor radius: 5D and longer time scales

How to construct a fluid model for the meso-scale solar wind?

One needs a **fluid model** that

- retains low-frequency kinetic effects: Landau damping and FLR corrections
(high frequency effects such as cyclotron resonance will be neglected)
- allows for background **temperature anisotropies**
- does not a priori order out the fast magnetosonic waves.
-> limits to standard (anisotropic) MHD at large scales.

Requirements: The model should

- reproduce the **linear properties of low-frequency waves**.
- ensure that the system **does not develop spurious instabilities at scales smaller than its range of validity**, and thus remains well-posed in the nonlinear regime.

Such a fluid model could also prove useful to provide **initial and/or boundary conditions for Vlasov simulations**.

The various fluid approaches

The main issues when writing a fluid model concerns the determination of the **pressure tensor**, and thus the order at which the fluid hierarchy is closed, and of the **Ohm's law**.

Pressure can be taken:

- such that the plasma is **cold**
- such that the flow remains **incompressible**
- scalar and **polytropic (isothermality is a special case)**
- scalar with an **energy equation**
- anisotropic but **bi-adiabatic**
- anisotropic but **taking into account heat fluxes** (with appropriate closure)
- anisotropic with **coupling to heat flux equations** (with appropriate closure on the 4th rank fluid moment)
- like above with the addition of **non-gyrotropic components** (FLR corrections)

Ohm's law can include:

- **$U \times B$ term only**: valid at MHD scales
- ion/electron decoupling at ion inertial scales : **Hall term** (monofluid)
- **electron pressure** contributions (important when $k p_e \approx (m_e/m_i)^{1/2}$)
- **electron inertia**, important close to electron inertial scales
- **diffusive term**, in the presence of collisions.
- or be replaced by a **bi-fluid** system for ions and electrons

Incompressible MHD

Drastic approximation, that assumes the presence of collisions; valid at very large scales.
Allows one to focus mainly on nonlinear phenomena.

Still many open problems:

The turbulent regime is not totally understood

(various theories : *Iroshnikov-Kraichnan 1965, Goldreich-Sridhar 1995, Perez & Boldyrev 2009*).

This model has many advantages:

Possibility to identify **two conserved quantities** ($\int (z^\pm)^2 \text{ where } z^\pm = u \pm b$)
which separately cascade towards small scales.

Existence of an **exact law**, analogous to the 4/5 law of Karman-Howarth
for homogeneous isotropic turbulence, giving statistics of 3rd order moments for
velocity increments (*Politano & Pouquet, GRL 25, 273; 1998*) and allowing
for the estimation of turbulent heating (Sorriso-Valvo et al. PRL **99**, 115001 (2007))

Reduced MHD

In the presence of a strong ambient field, the dynamics is essentially **decoupled**, even for finite beta, between:

- Incompressible MHD in the planes transverse to B_0
- Alfvén waves parallel to B_0

Derived originally for small β (*Rosenbluth et al. and Strauss PoF 1976*), it was later extended to more general cases.

Reduced MHD can be derived from gyrokinetic theory (Schekochihin, ApJ. sup. 2009).

To account for « temporal » dispersive effects at scales of the order or smaller than d_i :

Hall MHD

Replace Ohm's law $E = -U \times B$ by a more general expression.

After taking electron velocity equation, neglecting electron inertia, write:

$$\mathbf{E} + \mathbf{U} \times \mathbf{B} - \frac{1}{n_e e} \mathbf{J} \times \mathbf{B} + \frac{1}{n_e e} \nabla (n_e \kappa T_e) = \eta \mathbf{J}$$

If diffusive term and electron pressure are neglected:

$$E = -U_e \times B$$

Decoupling of electron and ion velocities.

The magnetic field however remains frozen in the electron flow.

With an ambient field and in the linear approximation: dispersive effects lead to separation of AWs into whistlers and ion cyclotron modes.

Incompressible limit only valid only in the **limit $\beta \rightarrow \infty$** (Sahraoui et al. JPP '07)

In the dispersive case, it is possible to derive a **4/5 law** (Galtier, PRE 77, 015302 (R); 2008) and to develop a theory of **weak turbulence** (Galtier, JPP 2006).

Both in the **weak turbulence** regime and in a **shell model** (Galtier and Buchlin ApJ 2007), incompressible Hall-MHD is able to capture a transition from an AW cascade at large scale, towards another type of cascade dominated by the **Hall nonlinearity**.

Transition at the ion inertial length: $d_i = v_A/\Omega$

In order to capture finite beta effects:

The compressible Hall-MHD model

$$\partial_t \rho + \nabla \cdot (\rho \mathbf{u}) = 0$$

$$\rho(\partial_t \mathbf{u} + \mathbf{u} \cdot \nabla \mathbf{u}) = -\frac{\beta}{\gamma} \nabla \rho^\gamma + (\nabla \times \mathbf{b}) \times \mathbf{b}$$

$$\partial_t \mathbf{b} - \nabla \times (\mathbf{u} \times \mathbf{b}) = -\frac{1}{R_i} \nabla \times \underbrace{\left(\frac{1}{\rho} (\nabla \times \mathbf{b}) \times \mathbf{b} \right)}_{\text{Hall term}}$$

$$\nabla \cdot \mathbf{b} = 0$$

Equation of state:

Isothermal ($\gamma=1$) when $V_{ph} \ll V_{th}$

Adiabatic when $V_{ph} \gg V_{th}$

In the presence of an ambient field, the Hall term induces dispersive effects.

Hall-MHD is a rigorous limit of collisionless kinetic theory for:

cold ions:

$$\begin{aligned} T_i &\ll T_e \\ \omega &\ll \Omega_i \\ k_{||} v_{thi} &\ll \omega \ll k_{||} v_{the} \end{aligned}$$

Irose et al., Phys. Lett. A 330, 474 (2004)
Ito et al., PoP 11, 5643 (2004)
Howes, NPG 16, 219 (2009)

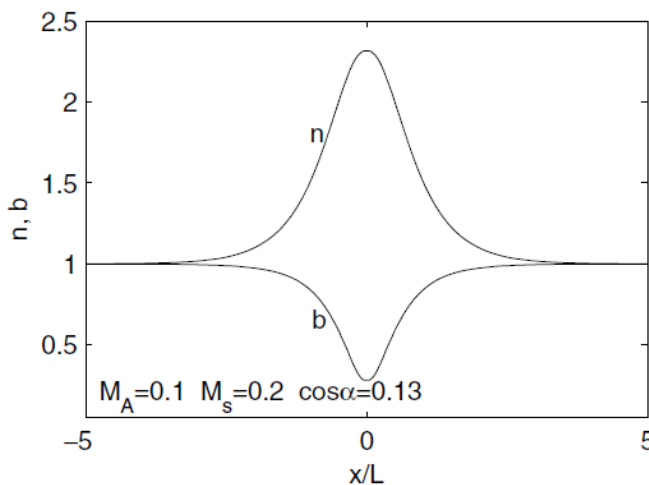
It correctly reproduces whistlers and KAW's for small to moderate β .



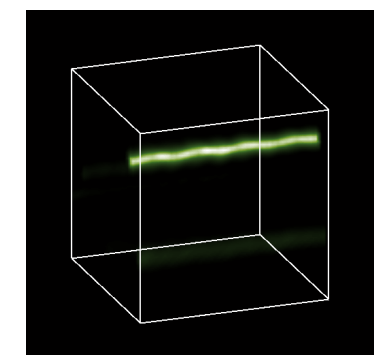
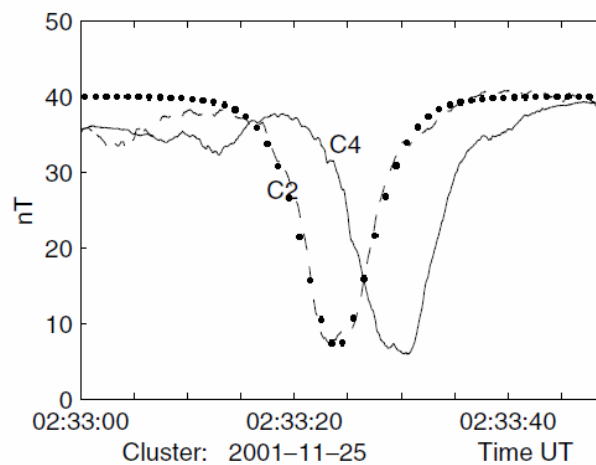
→ It contains waves that are usually damped in a collisionless plasma and whose influence in the turbulent dynamics has to be evaluated.

Compressibility introduces coupling to magnetosonic modes and allows for the presence of the decay instability for $\beta < 1$: important for the generation of contra-propagating Alfvén waves and thus the development of a cascade.

Dispersion can lead to solitonic structures:



Oblique soliton in Hall-MHD
(from Stasiewicz et al. PRL 2003)



but can also be the source of modulational instabilities and the formation of small scales: wave collapse:

Example: Alfvén wave **filamentation** in 3D Hall-MHD:

Laveder et al. PoP 9, 293; 2002

But compressible Hall-MHD lacks finite Larmor radius corrections, important for $\beta \sim 1$, and the correct dissipation of slow modes.

In order to capture **high frequency phenomena** and to break the magnetic field frozen-in condition: Introduce electron inertia.

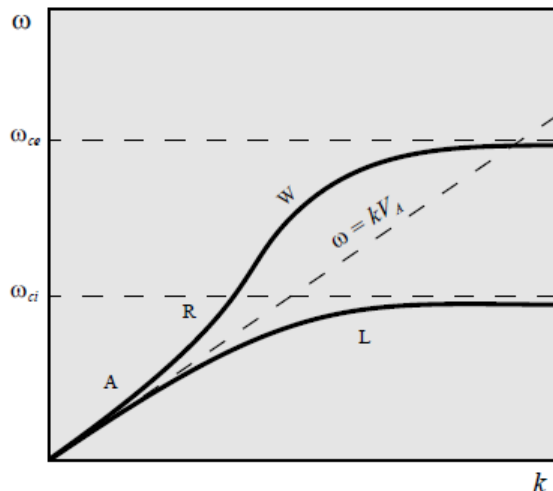
The bifluid model

Dynamical equations for the electron (and ion) velocity.

Allows one to study:

- **whistler** turbulence

(neglecting ion inertia the model can be simplified to so-called electron MHD; at small scales: ions are essentially immobile; currents are due to electrons)



- reconnection
no need to introduce dissipative mechanisms;
fast collisionless reconnection

Figure 8.12 Modes R et L ioniques : onde d'Alfvén.

Relax the **collisionallity assumption**: introduce a tensorial pressure and the so-called:

Che Goldberger Law (CGL) model or double adiabatic law

Chew et al., Proc. R. Soc. London A **236**, 112 , 1956

Assume a simple Ohm's law without Hall term and electron pressure gradient, and zero heat fluxes

Gyrotropy; tensor in the local frame: $\overleftrightarrow{\mathbf{P}}^{\text{MHD}} = \begin{bmatrix} P_{\perp} & 0 & 0 \\ 0 & P_{\perp} & 0 \\ 0 & 0 & P_{\parallel} \end{bmatrix} = P_{\perp} \overleftrightarrow{\mathbf{I}} + (P_{\parallel} - P_{\perp}) \widehat{\mathbf{B}} \widehat{\mathbf{B}}$

Conservation of adiabatic invariants:

$$\frac{P_{\parallel} B^2}{\rho^3} = \text{const.} \quad \frac{P_{\perp}}{\rho B} = \text{const.} \quad \text{along flow trajectories}$$

The **adiabatic** closure assumes that wave **phase speeds are much larger than particles thermal velocities** : it is not a proper closure for the solar wind.

For large enough temperature anisotropies, existence of **instabilities**.

Problem: CGL leads to wrong mirror threshold and does not provide stabilization at small scales

A MHD-like model for steady mirror structures

Although the mirror instability is driven by kinetic effects, some properties of stationary mirror structures can be captured within the anisotropic MHD, supplemented with a suitable equations of state: isothermal or static limit

A series of equations can be derived for the gyrotropic components of the even moments, and using the assumption of bi-Maxwellian distributions, simple equations of state can be obtained, which predicts the correct threshold of the mirror instability.

Consider the **static regime** characterized by a **zero hydrodynamic velocity** and **no time dependency of the other moments** (Passot, Ruban and Sulem, PoP 13, 102310, 2006).

Assume cold electrons (no parallel electric field)

Projecting the ion velocity equation along the local magnetic field (whose direction is defined by the unit vector \hat{b}) leads to the **parallel pressure equilibrium condition**

$$\hat{b}_m \frac{\partial}{\partial x_n} P_{mn} = 0$$

for the (gyrotropic) pressure tensor $P_{ij} = p_\perp n_{ij} + p_\parallel \tau_{ij}$

where $n_{ij} = \delta_{ij} - \hat{b}_i \hat{b}_j$ and $\tau_{ij} = \hat{b}_i \hat{b}_j$ are the fundamental gyrotropic tensors.

The above condition rewrites: $(\hat{b} \cdot \nabla) p_\parallel + (p_\parallel - p_\perp) \nabla \cdot \hat{b} = 0$.

From the divergenceless of $\mathbf{B} = B \hat{b}$, one has $\frac{1}{\nabla \cdot \hat{b}} \hat{b} \cdot \nabla = - \frac{B}{\hat{b} \cdot \nabla B} \hat{b} \cdot \nabla = - \bar{B} \frac{d}{d\bar{B}} = - \frac{d}{dX}$,
with $X = \ln \bar{B}$.

This leads to the condition

$$\frac{dp_\parallel}{dX} = p_\parallel - p_\perp.$$

We proceed in a similar way at the level of the equation for [the heat flux tensor](#), by contracting with the two fundamental tensors τ_{ij} and n_{ij} , and get

$$\hat{b}_l \tau_{ij} \frac{\partial}{\partial x_k} R_{ijkl} = 0,$$

$$\hat{b}_l n_{ij} \frac{\partial}{\partial x_k} R_{ijkl} = 0,$$

where the 4th-order moment is taken in the gyrotropic form

$$R_{ijkl} = r_{\parallel\parallel} \tau_{ij} \tau_{kl} + r_{\parallel\perp} \mathcal{S}\{n_{ij} \tau_{kl}\} + r_{\perp\perp} \mathcal{S}\{n_{ij} n_{kl}\}.$$

Here, \mathcal{S} refers to the symmetrization with respect to all the indices. One gets

$$\frac{dr_{\parallel\parallel}}{dX} = r_{\parallel\parallel} - 3r_{\parallel\perp},$$

$$\frac{dr_{\parallel\perp}}{dX} = 2r_{\parallel\perp} - r_{\perp\perp}.$$

The **closure** then consists in assuming that the 4th-order moments are related to the second order ones as in the case of a bi-Maxwellian distribution, i.e.:

$$r_{\parallel\parallel} = 3p_{\parallel}^2/\rho$$

$$r_{\parallel\perp} = p_{\parallel}p_{\perp}/\rho$$

and

$$r_{\perp\perp} = 2p_{\perp}^2/\rho$$

Closure can be done at higher order

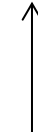
One finally gets

$$\begin{cases} \frac{d\bar{T}_{\parallel}}{dX} = 0, \\ \frac{d\bar{T}_{\perp}}{dX} = \bar{T}_{\perp} \left[1 - (A + 1) \frac{\bar{T}_{\perp}}{\bar{T}_{\parallel}} \right]. \end{cases}$$

These equations are solved as

$$A = (\bar{T}_{\perp}^{(0)} / \bar{T}_{\parallel}^{(0)}) - 1$$

$$\bar{T}_{\parallel} = 1, \quad \bar{T}_{\perp} = \frac{\bar{B}}{(A + 1)\bar{B} - A}$$



« Initial condition »
at $X=0$

Similar equations of state were derived using a fully kinetic argument by Constantinescu, J. Atmos. Terr. Phys. **64**, 645 (2002).

Equations actually also valid with warm electrons

FLR-Landau fluid

Fluid model retaining *Hall effect*, *Landau damping* and *ion finite Larmor radius (FLR) corrections in the sub-ion range*. Electron FLR corrections and electron inertia neglected.

Landau fluids were first introduced by *Hammett & Perkins (PRL 64, 3019, 1990)* as a closure retaining linear Landau damping.

The FLR-LF is an extension of the Landau fluid for MHD scales derived in *Snyder, Hammett & Dorland, Phys. Plasmas 4, 3974, 1997*.

The fluid hierarchy for the gyrotropic moments is closed by evaluating the gyrotropic 4th rank cumulants and the non-gyrotropic contributions to all the retained moments, in a way **consistent with the linear kinetic theory, within a low-frequency asymptotics**.

The model reproduces dispersion and damping rate of low-frequency modes at the sub-ion scales.

References:

Passot & Sulem, Phys. Plasmas 14, 082502, (2007); Passot, Sulem & Hunana, Phys. Plasmas 19, 082113, (2012); Sulem & Passot, J. Plasma Phys. 81 (1), 32810103 (2015)

First 3D FLR-LF simulations of turbulence at ionic scales presented in
Passot, Henri, Laveder & Sulem, Eur. Phys. J. D. 68, 207, 2014.
see also
Sulem, Passot, Laveder & Borgogno, ApJ 816:66 (2016).

Alternative approach: gyrofluids

(Brizard 1992, Dorland & Hammett 1993, Beer & Hammett 1996)

- Obtained by taking velocity moments of the gyrokinetic equation.
- Nonlinear FLR corrections to all orders are captured.
- Linear closure of the hierarchy needed as for Landau fluids.
- All fast magnetosonic waves are ordered out: transverse velocity expressed in drift approximation.

Both Landau fluids and gyrofluids neglect wave particle trapping, i.e. the effect of particle bounce motion on the distribution function near resonance.

The FLR-Landau fluid model

For the sake of simplicity, neglect electron inertia.

Ion dynamics: derived by computing velocity moments from Vlasov Maxwell equations.

$$\left\{ \begin{array}{l} \partial_t \rho_p + \nabla \cdot (\rho_p u_p) = 0 \\ \partial_t u_p + u_p \cdot \nabla u_p + \frac{1}{\rho_p} \nabla \cdot \mathbf{p}_p - \frac{e}{m_p} (E + \frac{1}{c} u_p \times B) = 0 \\ E = -\frac{1}{c} \left(u_p - \frac{j}{ne} \right) \times B - \frac{1}{ne} \nabla \cdot \mathbf{p}_e, \\ \partial_t B = -c \nabla \times E \end{array} \right. \quad \begin{array}{l} \rho_r = m_r n_r \\ \text{quasi-neutrality } (n_e = n_p) \\ \text{Not relativistic: no displacement current} \\ j = \frac{c}{4\pi} \nabla \times \mathbf{B} \end{array}$$

pressure tensor $P_r = m_r n_r \int (v - u_r) \otimes (v - u_r) f_r d^3 v$

heat flux tensor $Q_r = m_r n_r \int (v - u_r) \otimes (v - u_r) \otimes (v - u_r) f_r d^3 v$.

$$\partial_t \mathbf{P}_r + u_r \cdot \nabla \mathbf{P}_r + \mathbf{P}_r \nabla \cdot u_r + \nabla \cdot \mathbf{Q}_r + [\mathbf{P}_r \cdot \nabla u_r + \frac{q_r}{m_r c} b \times \mathbf{P}_r]^S = \mathbf{H}_r$$

$$\mathbf{u}_e = \mathbf{u}_p - \mathbf{j}/ne$$

zero in the absence of collisions

where the tensor $B \times \mathbf{p}_r$ has elements $(B \times \mathbf{p}_r)_{ij} = \epsilon_{iml} B_m p_{rlj}$

The pressure tensor is decomposed as follows:

FLR corrections

\downarrow

$$\mathbf{p}_p = p_{\perp p} \mathbf{n} + p_{\parallel p} \boldsymbol{\tau} + \boldsymbol{\Pi}, \text{ with } \mathbf{n} = \mathbf{I} - \hat{\mathbf{b}} \otimes \hat{\mathbf{b}} \text{ and } \boldsymbol{\tau} = \hat{\mathbf{b}} \otimes \hat{\mathbf{b}}, \text{ where } \hat{\mathbf{b}} = \mathbf{B} / |\mathbf{B}|.$$

Electron pressure tensor is taken gyrotropic
(considered scales \gg electron Larmor radius)
and thus characterized by the parallel and transverse pressures $p_{\parallel e}$ and $p_{\perp e}$.

Exact equations for the perpendicular and parallel pressures

$$\partial_t p_{\perp r} + \nabla \cdot (\vec{u}_r p_{\perp r}) + p_{\perp r} \nabla \cdot \vec{u}_r - p_{\perp r} \hat{b} \cdot \nabla \vec{u}_r \cdot \hat{b} + \frac{1}{2} \left(\text{tr } \nabla \cdot \mathbf{q}_r - \hat{b} \cdot (\nabla \cdot \mathbf{q}_r) \cdot \hat{b} \right) \\ + \frac{1}{2} \left(\text{tr } (\boldsymbol{\Pi} \cdot \nabla \vec{u})^S - (\boldsymbol{\Pi} \cdot \nabla \vec{u})^S : \boldsymbol{\tau} + \boldsymbol{\Pi} : \frac{d\boldsymbol{\tau}}{dt} \right)_r \delta_{rp} = 0$$

$$\partial_t p_{\parallel r} + \nabla \cdot (\vec{u}_r p_{\parallel r}) + 2p_{\parallel r} \hat{b} \cdot \nabla \vec{u}_r \cdot \hat{b} + \hat{b} \cdot (\nabla \cdot \mathbf{q}_r) \cdot \hat{b} \\ + \left((\boldsymbol{\Pi} \cdot \nabla \vec{u})^S : \boldsymbol{\tau} - \boldsymbol{\Pi} : \frac{d\boldsymbol{\tau}}{dt} \right)_r \delta_{rp} = 0,$$

heat flux tensor

work of the non-gyrotropic pressure force

Modelization of the heat flux tensor:

$$\mathbf{q}_r = \mathbf{S}_r + \boldsymbol{\sigma}_r \quad \text{with} \quad \boldsymbol{\sigma}_r : \mathbf{n} = 0 \text{ and } \boldsymbol{\sigma}_r : \boldsymbol{\tau} = 0.$$

The tensor \mathbf{S} writes:

$$S_{ijk} = \frac{1}{2} (S_i^\perp n_{jk} + S_j^\perp n_{ik} + S_k^\perp n_{ij} + S_l^\perp \tau_{li} n_{jk} + S_l^\perp \tau_{lj} n_{ik} + S_l^\perp \tau_{lk} n_{ij}) \\ + S_i^\parallel \tau_{jk} + S_j^\parallel \tau_{ik} + S_k^\parallel \tau_{ij} - \frac{2}{3} (S_l^\parallel \tau_{li} \tau_{jk} + S_l^\parallel \tau_{lj} \tau_{ik} + S_l^\parallel \tau_{lk} \tau_{ij}),$$

The vectors \mathbf{S}^\parallel and \mathbf{S}^\perp are defined by

$$\vec{S}_r^\parallel = \mathbf{q}_r : \boldsymbol{\tau} \quad \text{and} \quad \vec{S}_r^\perp = \mathbf{q}_r : \mathbf{n} / 2.$$

One has $q_{\perp r} = \vec{S}_r^\perp \cdot \hat{b}$ and $q_{\parallel r} = \vec{S}_r^\parallel \cdot \hat{b}$.

They are the only contributions to the gyrotropic heat flux tensor:

$$q_r^G{}_{ijk} = q_{\parallel r} \hat{b}_i \hat{b}_j \hat{b}_k + q_{\perp r} (\delta_{ij} \hat{b}_k + \delta_{ik} \hat{b}_j + \delta_{jk} \hat{b}_i - 3 \hat{b}_i \hat{b}_j \hat{b}_k).$$

One can write $\vec{S}_r^\perp = q_{\perp r} \hat{b} + \vec{S}_{\perp r}^\perp$ and $\vec{S}_r^\parallel = q_{\parallel r} \hat{b} + \vec{S}_{\perp r}^\parallel$.

The contribution of the tensor S in the pressure equations then reads:

$$\begin{aligned} \hat{b} \cdot (\nabla \cdot \mathbf{S}_r) \cdot \hat{b} &= \nabla \cdot (q_{\parallel r} \hat{b} + \vec{S}_{\perp r}^\parallel) - 2q_{\perp r} \nabla \cdot \hat{b} - 2\hat{b} \cdot \nabla \hat{b} \cdot \vec{S}_r^\parallel \\ \frac{1}{2} \left(\text{tr}(\nabla \cdot \mathbf{S}_r) - \hat{b} \cdot (\nabla \cdot \mathbf{S}_r) \cdot \hat{b} \right) &= \nabla \cdot (q_{\perp r} \hat{b} + \vec{S}_{\perp r}^\perp) + q_{\perp r} \nabla \cdot \hat{b} + \hat{b} \cdot \nabla \hat{b} \cdot \vec{S}_r^\parallel \end{aligned}$$

At the linear level, σ_r does not contribute to the heat flux terms in the equations for the gyrotropic pressures.

Nonlinear expressions of σ_r in the large-scale limit given in *Ramos, PoP 12, 052102 (2005)*

Equations for the perpendicular and parallel gyrotropic heat fluxes

At this level some simplifications are introduced to reduce the level of complexity
(see Ramos 2005 for the full set of nonlinear equations)

Terms that involve the non-gyrotropic pressure and heat fluxes are kept only when they appear **linearly**

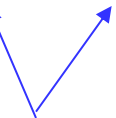
$$\partial_t q_{\parallel r} + \nabla \cdot (q_{\parallel r} \vec{u}_r) + 3q_{\parallel r} \hat{\vec{b}} \cdot \nabla \vec{u}_r \cdot \hat{\vec{b}} + 3p_{\parallel r} (\hat{\vec{b}} \cdot \nabla) \left(\frac{p_{\parallel r}}{\rho} \right)$$

$$+ \nabla \cdot (\tilde{r}_{\parallel \parallel r} \hat{\vec{b}}) - 3\tilde{r}_{\parallel \perp r} \nabla \cdot \hat{\vec{b}} + R_{\parallel r}^{NG} = 0$$

$$\partial_t q_{\perp r} + \nabla \cdot (\vec{u}_r q_{\perp r}) + q_{\perp r} \nabla \cdot \vec{u}_r + p_{\parallel r} (\hat{\vec{b}} \cdot \nabla) \left(\frac{p_{\perp r}}{\rho} \right) + \delta_{rp} \frac{p_{\perp r}}{\rho} \left(\partial_x \Pi_{xz} + \partial_y \Pi_{yz} \right)_r$$

$$+ \nabla \cdot (\tilde{r}_{\parallel \perp r} \hat{\vec{b}}) + \left((p_{\parallel r} - p_{\perp r}) \frac{p_{\perp r}}{\rho} - \tilde{r}_{\perp \perp r} + \tilde{r}_{\parallel \perp r} \right) (\nabla \cdot \hat{\vec{b}}) + R_{\perp r}^{NG} = 0,$$

Involve the 4th-rank gyrotropic cumulants: $\tilde{r}_{\parallel \parallel}, \tilde{r}_{\parallel \perp}, \tilde{r}_{\perp \perp}$



R_{\parallel}^{NG} and R_{\perp}^{NG}

stand for the linear **nongyrotropic contributions** of the 4th-rank cumulants.

$$\begin{cases} \tilde{r}_{\parallel \parallel} = r_{\parallel \parallel} - 3 \frac{p_{\parallel}^2}{\rho}, \\ \tilde{r}_{\parallel \perp} = r_{\parallel \perp} - \frac{p_{\perp} p_{\parallel}}{\rho}, \\ \tilde{r}_{\perp \perp} = r_{\perp \perp} - 2 \frac{p_{\perp}^2}{\rho}. \end{cases}$$

The completion of this model requires the determination of:

- closure relations to express the 4th-rank cumulants $\tilde{r}_{\parallel\parallel}, \tilde{r}_{\parallel\perp}, \tilde{r}_{\perp\perp}$
(closure at lower or higher order also possible)

Only issue when dealing with the Large-Scale Landau fluid model
(*Snyder, Hammett & Dorland, PoP 4, 3974, 1997*).

- (non gyrotropic) FLR corrections to all moments.

A quasi-normal closure (obtained by taking $\tilde{r}_{\parallel\parallel}, \tilde{r}_{\parallel\perp}, \tilde{r}_{\perp\perp}$ zero)
and with no FLRs leads to a system that does not include
any form of dissipation.

In the limit of zero collisions, fluid equations nevertheless contain a finite
dissipation, associated to **the phase mixing** process.

Phase mixing

(from Hammett et al. *Phys. Fluid B4*, 2052, 1992)

$$\frac{\partial f}{\partial t} + v \frac{\partial f}{\partial z} = \delta(t) f_0(z, v), \quad \text{exact solution: } f(z, v, t) = f_0(z - vt, v) H(t)$$

Consider $f_0(z, v) = (n_0 + n_1 e^{ikz}) f_M(v)$.

Then $f(z, v, t) = (n_0 + n_1 e^{ik(z-vt)}) (1/\sqrt{2\pi v_t^2}) e^{-v^2/(2v_t^2)}$. (No damping)

Take the first moment (density):

$$n(z, t) = \int dv f = n_0 + n_1 \underbrace{\frac{e^{ikz}}{\sqrt{2\pi v_t^2}}}_{\substack{\text{mixing}}} \underbrace{\int dv e^{-ikvt}}_{\text{phase}} e^{-v^2/(2v_t^2)}.$$

Hence

$$n_1(t) = n_1(0) e^{-k^2 v_t^2 t^2 / 2}$$

Time decay!

How to introduce the proper form of dissipation in the fluid system?

Simplest possible closure for the electrostatic problem $\frac{\partial f}{\partial t} + v \frac{\partial f}{\partial z} + \frac{e}{m} E \frac{\partial f}{\partial v} = 0,$

Taking the mass conservation equation $\frac{\partial n}{\partial t} + \frac{\partial}{\partial z} (un) = 0,$

one can impose a Fick's law of diffusion by imposing the higher moment u in terms of the previous moment n in the form

$$un \approx -D \frac{\partial n}{\partial z},$$

Then $n_1(t) = n_1(0) \exp(-Dk^2t).$

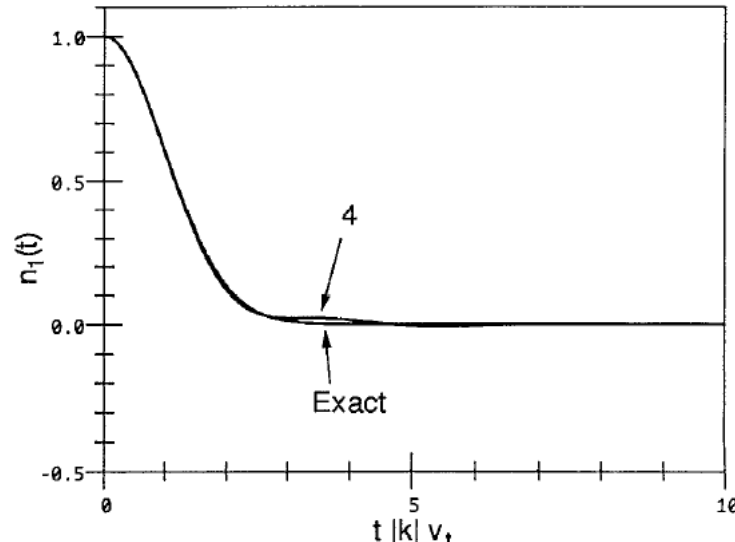
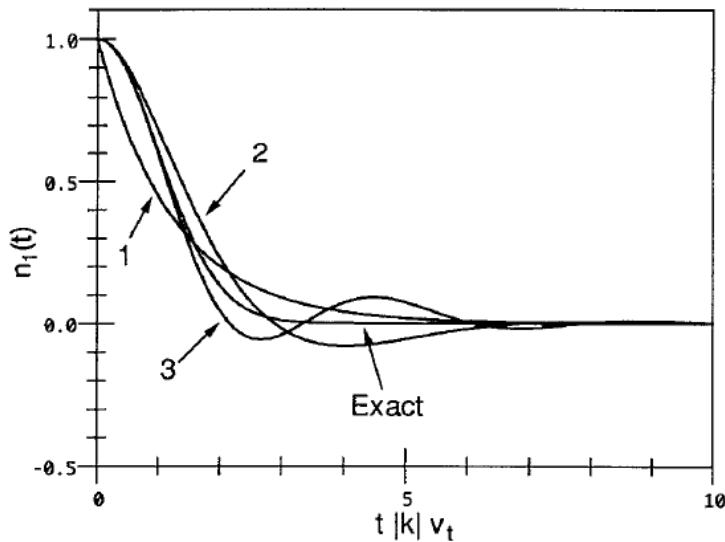
Taking $D = \sqrt{(2/\pi)}(v_t/|k|)$. ensures the proper decay law.

The particle flux that in Fourier space reads $\Gamma_k = -D_k \frac{\partial n}{\partial z}$ rewrites

$$\Gamma(z) = -\frac{2^{1/2} v_t}{\pi^{3/2}} \int_0^\infty dz' \frac{n(z+z') - n(z-z')}{z'}$$

It is a nonlocal operator (Hilbert transform) along field lines

The agreement with kinetic theory is better as the number of fluid moments is increased.



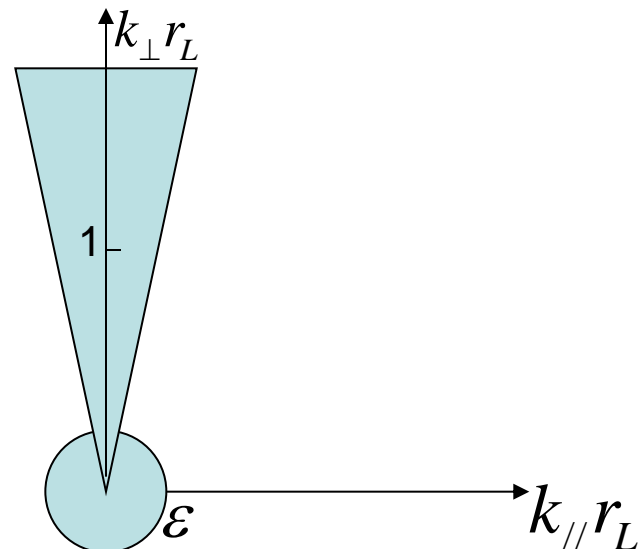
Closure for the FLR-LF model at the level of energy-weighted pressures

Calculate the 4th-rank cumulants **from the linearized kinetic theory**,
in the low-frequency limit: (for a bi-Maxwellian d.f.) $\omega/\Omega \sim \epsilon \ll 1$

In this case, the expansion is valid for:

- quasi-transverse fluctuations $(k_{\parallel}/k_{\perp} \sim \epsilon)$ with $k_{\perp}r_L \sim 1$
- hydrodynamic scales with $k_{\parallel}r_L \sim k_{\perp}r_L \sim \epsilon$.

r_L : ion Larmor radius



$$r_L^2 = \frac{v_{th\perp}^2}{\Omega^2} = \frac{2T_{\perp}}{m_i\Omega^2}$$

The kinetic expressions typically depend on electromagnetic field components and involve the plasma dispersion function (which is nonlocal both in space and time).

These various expressions are expressed in terms of other fluid moments in such a way as to minimize the occurrence of the plasma dispersion function.

The latter is otherwise replaced by suitable Padé approximants, thus leading to local-in-time expressions. At some places, a Hilbert transform with respect to the longitudinal space coordinate appears, that modelizes Landau damping.

This procedure ensures consistency with the low-frequency linear kinetic theory, up to the use of Padé approximants.

Hierarchy closure

from kinetic theory:

R: plasma response function

$$\zeta = (\omega / |k_z|) \sqrt{m / 2T_{\parallel}^{(0)}}$$

$$b = T_{\perp}^{(0)} k_{\perp}^2 / m\Omega^2 = k_{\perp}^2 r_L^2 / 2$$

Larmor radius

$$\Gamma_{\nu}(b) = e^{-b} I_{\nu}(b)$$

Bessel modified function

At scales >> Larmor radius

$$\Gamma_0(b) = 1 \quad \Gamma_1(b) = 0$$

For each species

$$\left\{ \begin{array}{l} \tilde{r}_{\parallel\parallel} = \frac{p_{\parallel}^{(0)} T_{\perp}^{(0)}}{m} \{ 2\zeta^2 [1 + 2\zeta^2 R(\zeta)] + 3[R(\zeta) - 1] - 12\zeta^2 R(\zeta) \} \\ \quad \times \left\{ [\Gamma_1(b) - \Gamma_0(b)] \frac{b_z}{B_0} - \Gamma_0(b) \frac{e\Psi}{T_{\perp}^{(0)}} \right\} \\ \\ \tilde{r}_{\parallel\perp} = \frac{p_{\perp}^{(0)2}}{\rho^{(0)}} [1 - R(\zeta) + 2\zeta^2 R(\zeta)] \left\{ [2b\Gamma_0(b) - \Gamma_0(b) \right. \\ \quad \left. - 2b\Gamma_1(b)] \frac{b_z}{B_0} + b[\Gamma_0(b) - \Gamma_1(b)] \frac{e\Psi}{T_{\perp}^{(0)}} \right\} \end{array} \right.$$

These formulas can be expressed in terms of lower order fluid moments.

Using 4-pole Padé:

$$R_4(\zeta) = \frac{4 - 2i\sqrt{\pi}\zeta + (8 - 3\pi)\zeta^2}{4 - 6i\sqrt{\pi}\zeta + (16 - 9\pi)\zeta^2 + 4i\sqrt{\pi}\zeta^3 + (6\pi - 16)\zeta^4},$$

one gets:

$$\tilde{r}_{\parallel\parallel r} = \frac{32 - 9\pi}{2(3\pi - 8)} n_0 v_{\text{th}\parallel r}^2 T'_{\parallel r} - \frac{2\sqrt{\pi}}{3\pi - 8} v_{\text{th}\parallel r} H q_{\parallel r}$$

Using 2-pole Padé:

$$R_2(\zeta) = 1 / (1 - i\sqrt{\pi}\zeta - 2\zeta^2)$$

In physical space:
negative Hilbert
transform: signature
of Landau resonance

overline: instantaneous
space average
prime: fluctuations

$$\text{one gets: } \tilde{r}_{\parallel\perp p} = -\frac{\sqrt{\pi}}{2} v_{\text{th}\parallel p} H \left[q_{\perp p} + \frac{v_{\text{th}\parallel p}^2}{2\Omega_p} \frac{\bar{T}_{\perp p}}{\bar{T}_{\parallel p}} (\bar{p}_{\perp p} - \bar{p}_{\parallel p}) \widehat{\mathcal{R}_{\parallel\perp}} \left(\nabla \wedge \frac{\mathbf{B}}{B_0} \right) \cdot \mathbf{b} \right]$$

$$\tilde{r}_{\parallel\perp e} = -\frac{\sqrt{\pi}}{2} v_{\text{th}\parallel e} H \left[q_{\perp e} - \frac{v_{\text{th}\parallel e}^2}{2\Omega_p} \frac{\bar{T}_{\perp e}}{\bar{T}_{\parallel p}} (\bar{p}_{\perp e} - \bar{p}_{\parallel e}) \left(\nabla \wedge \frac{\mathbf{B}}{B_0} \right) \cdot \mathbf{b} \right]$$

at large scales $\tilde{r}_{\perp\perp} = 0$

How to deal with the operator H?

Accurately retaining the magnetic field distortion requires the replacement of the Hilbert transform along the ambient field by an integral along the individual magnetic field lines, which is hardly feasible on the present day computers.

Replace H by: $\widehat{[(\mathbf{k} \cdot \bar{\tau} \cdot \mathbf{k})^{-\frac{1}{2}}]} \partial_{\parallel}$ ($\partial_{\parallel} = \mathbf{b} \cdot \nabla$)

where $\bar{\tau}$ is the instantaneous space average of τ

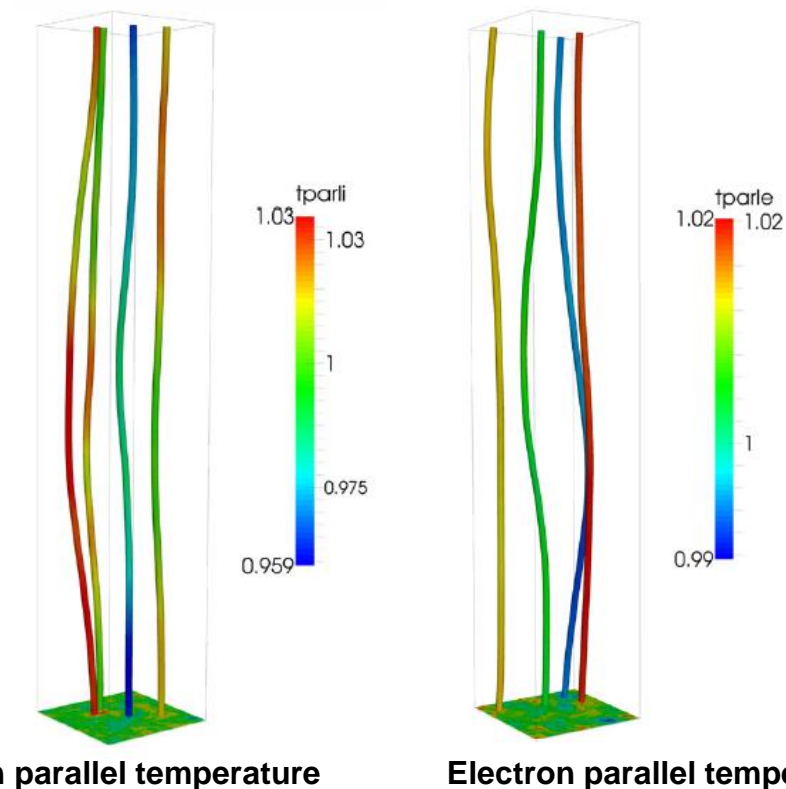
It preserves the zero-th order character of this operator.

It is exact in the linear limit (whatever the direction of the ambient field).

It is generically non-singular on the numerical grid.

Temperature homogenization along field lines is more efficient for electrons.

Temperature can however vary significantly from one field line to the other.



At which **level** is it appropriate to close the hierarchy?

Keeping higher fluid moments allows one to account for distortions of the distribution function and to keep more fluid nonlinearities.

It also better mimick the cascade in velocity space with a possible stochastic plasma echo (Schekochihin et al. JPP **82**, 905820212, 2016)

Taking a higher order Padé approximant leads to more precise approximations. But, except in particular cases, all the ζ terms cannot be eliminated, thus leading to closure relations in the form of linear PDEs instead of algebraic relations.

This is thus analogous to closing the fluid hierarchy at a higher moment, possibly with a Padé of lower order $\tilde{r}_{\parallel \perp}$

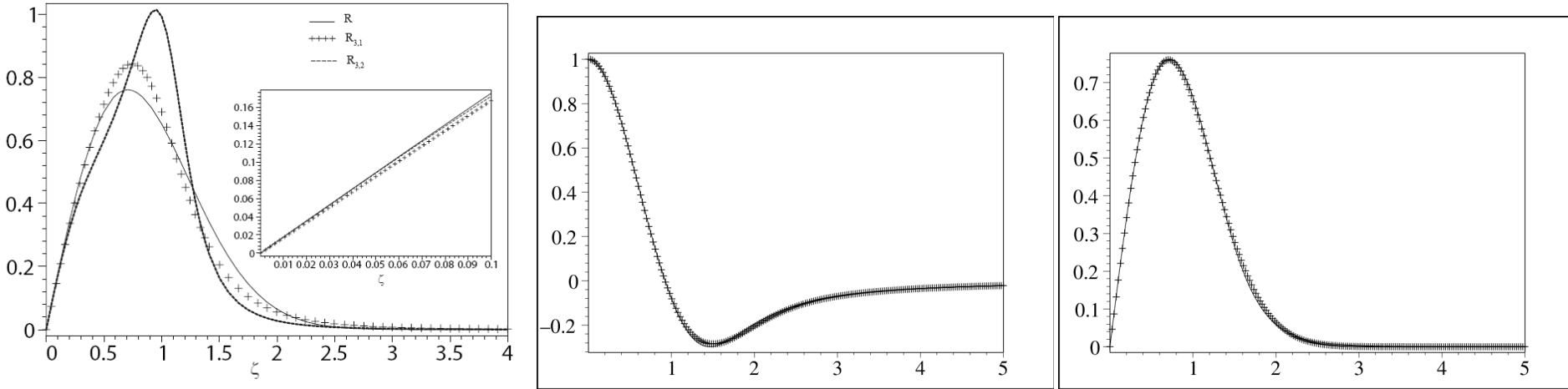


FIG. 1: Comparison between the imaginary part of the function $R(\zeta)$ (thin solid line) with the corresponding Padé approximants $R_{3,1}$ (crosses) and $R_{3,2}$ (thick dashed line). The insert displays the same quantities in a smaller range of ζ , close to the origin.

Imaginary part for R_3

Real part for R_4

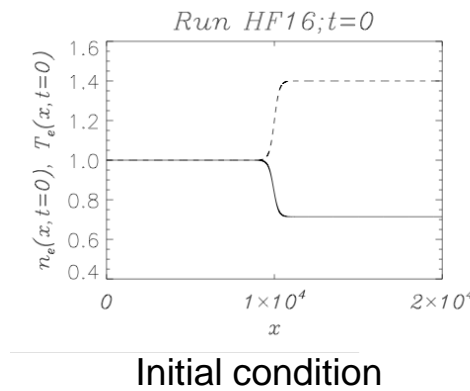
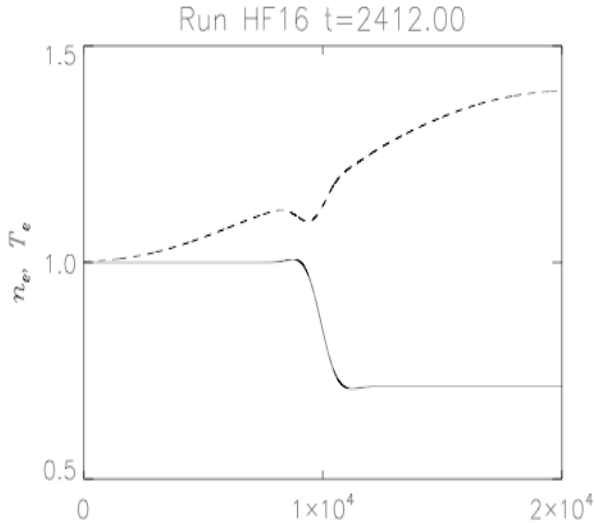
Imaginary part for R_4

Several choices of Padé approximant are possible.
 For the case of the three-pole Padé, we choose one that
 has a globally better fit, even if another one performs
 slightly better at large scales. The four-pole Padé appears excellent
 throughout the whole range of ζ .

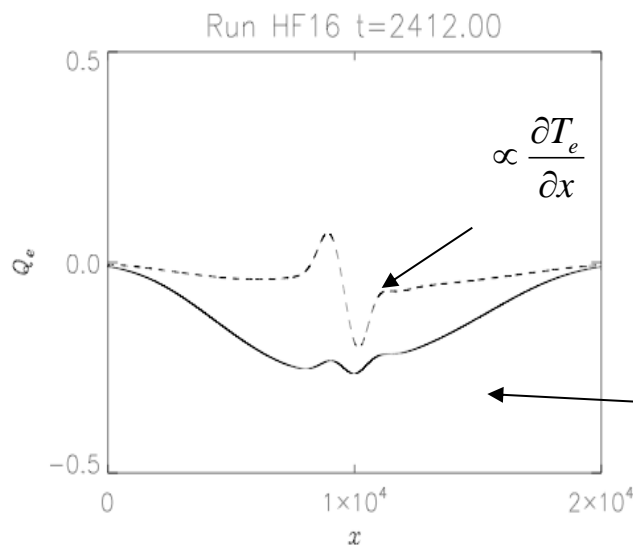
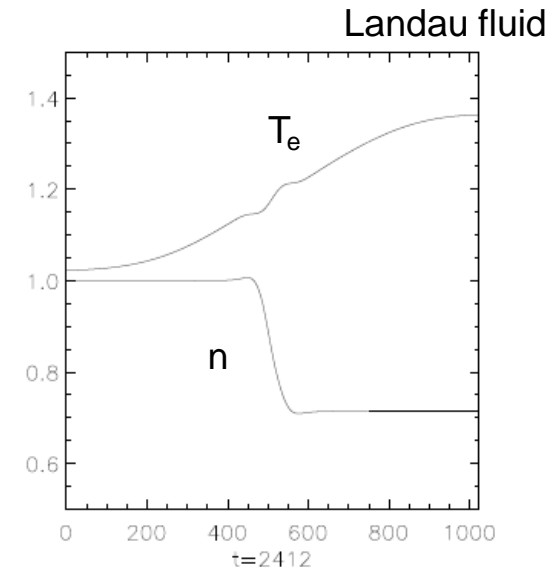
Diffusion of a temperature gradient

Comparaison between Vlasov and Landau fluid simulations

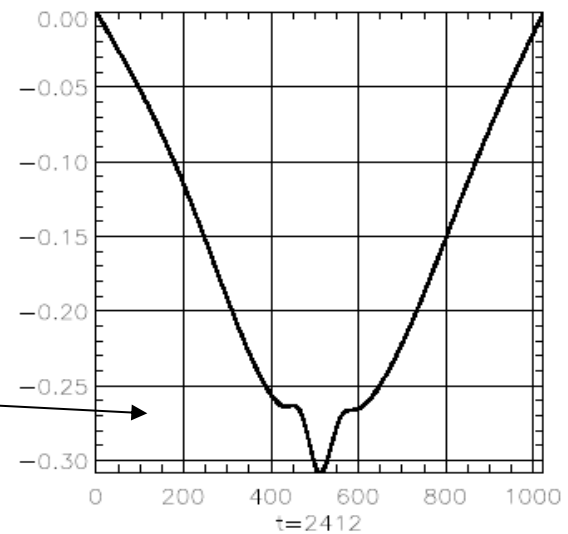
Vlasov (A. Mangeney and F. Califano)



Domain size:
20 000 λ_e



Parallel electron
heat flux



Two methods to determine the non-gyrotropic elements of the tensors

- I. Solve the (coupled) algebraic equations that result from the projection the tensorial pressure equations, orthogonally to the gyrotropic "directions".

At the level of the pressure:

$$\nabla_r \rightarrow \mathbf{P}_r \times \hat{\mathbf{b}} - \hat{\mathbf{b}} \times \mathbf{P}_r = \mathbf{k}_r$$

$$\mathbf{k}_r = \frac{1}{\Omega_r} \frac{B_0}{|b|} \left[\frac{d\mathbf{P}_r}{dt} + (\nabla \cdot u_r) \mathbf{P}_r + \nabla \cdot \mathbf{Q}_r + (\mathbf{P}_r \cdot \nabla u_r)^S \right].$$

The left hand side $\mathbf{P}_r \times \hat{\mathbf{b}} - \hat{\mathbf{b}} \times \mathbf{P}_r$ can be viewed as a self-adjoint linear operator acting on \mathbf{P}_r , whose kernel is spanned by the tensors $(\mathbf{I} - \hat{\mathbf{b}} \otimes \hat{\mathbf{b}})$ and $\hat{\mathbf{b}} \otimes \hat{\mathbf{b}}$.

The solvability conditions lead to the dynamical equations for pressures and heat fluxes

Since Π also appears in the r.h.s., this procedure requires an expansion in a small parameter, usually taken as the time and space scale separation with the ion gyroscales.

It follows that (see e.g. Schekochihin et al. MNRAS **405**, 291–300 (2010) for a simple derivation) :

$$\Pi = \frac{1}{4\Omega_p^L} [\mathbf{b} \wedge \mathbf{W} \cdot (\mathbf{I} + 3\tau) - (\mathbf{I} + 3\tau) \cdot \mathbf{W} \wedge \mathbf{b}] + \frac{1}{\Omega_p^L} [\mathbf{b} \otimes (\mathbf{w} \wedge \mathbf{b}) + (\mathbf{w} \wedge \mathbf{b}) \otimes \mathbf{b}].$$

with: $\mathbf{W} = [p_{\perp p} \nabla \mathbf{u}_p + \nabla (q_{\perp p} \mathbf{b})]^S$

$$\mathbf{w} \wedge \mathbf{b} = [2(p_{\perp p} - p_{\parallel p}) \partial_{\parallel} \mathbf{u}_p + (3q_{\perp p} - q_{\parallel p}) \partial_{\parallel} \mathbf{b}] \wedge \mathbf{b}.$$

and also for the heat fluxes (only the S terms for the protons are displayed):

$$S_{\perp p}^{\perp} = \frac{1}{\Omega_p^L} \mathbf{b} \wedge \left[2 \frac{p_{\perp p}}{m_p} \nabla T_{\perp p} + 4q_{\perp p} \partial_{\parallel} \mathbf{u}_p + 2\tilde{r}_{\parallel \perp} \partial_{\parallel} \mathbf{b} \right]$$

$$S_{\perp p}^{\parallel} = \frac{1}{\Omega_p^L} \mathbf{b} \wedge \left[\frac{p_{\perp p}}{m_p} \nabla T_{\parallel p} + 2 \frac{T_{\parallel p}}{m_p} (p_{\parallel p} - p_{\perp p}) \partial_{\parallel} \mathbf{b} + 2q_{\parallel p} \partial_{\parallel} \mathbf{u}_p + 2q_{\perp p} (\mathbf{b} \wedge \boldsymbol{\omega}_p) + \nabla \tilde{r}_{\parallel \perp p} + (\tilde{r}_{\parallel \parallel p} + 3\tilde{r}_{\parallel \perp p}) \partial_{\parallel} \mathbf{b} \right].$$

A large-scale model is obtained with closures of the form

$$q_{\parallel r} = -\bar{p}_{\parallel r} v_{\text{th}\parallel r} \frac{2}{\sqrt{\pi}} H \frac{T_{\parallel r}}{\bar{T}_{\parallel r}}$$

$$\begin{aligned} q_{\perp p} = & -\frac{\bar{p}_{\perp p}}{\Omega_p} \frac{(\bar{T}_{\perp p} - \bar{T}_{\parallel p})}{m_p} \mathbf{b} \cdot \left(\nabla \wedge \frac{\mathbf{B}}{B_0} \right) - \bar{p}_{\perp p} v_{\text{th}\parallel p} \\ & \times \frac{H}{\sqrt{\pi}} \left[\frac{T_{\perp p}}{\bar{T}_{\perp p}} - \frac{1}{\Omega_p} \mathbf{b} \cdot (\nabla \wedge \mathbf{u}_p) + \left(\frac{\bar{T}_{\perp p}}{\bar{T}_{\parallel p}} - 1 \right) \frac{|\mathbf{B}|}{B_0} \right] \end{aligned}$$

$$q_{\perp e} = \frac{\bar{p}_{\perp e}}{\Omega_p} \frac{(\bar{T}_{\perp e} - \bar{T}_{\parallel e})}{m_p} \mathbf{b} \cdot \left(\nabla \wedge \frac{\mathbf{B}}{B_0} \right) - \bar{p}_{\perp e} v_{\text{th}\parallel e} \frac{H}{\sqrt{\pi}} \left[\frac{T_{\perp e}}{\bar{T}_{\perp e}} + \left(\frac{\bar{T}_{\perp e}}{\bar{T}_{\parallel e}} - 1 \right) \frac{|\mathbf{B}|}{B_0} \right]$$

$$\tilde{r}_{\parallel\parallel p} = -\frac{3}{2} n_0 v_{\text{th}\parallel r}^2 T'_{\parallel p}$$

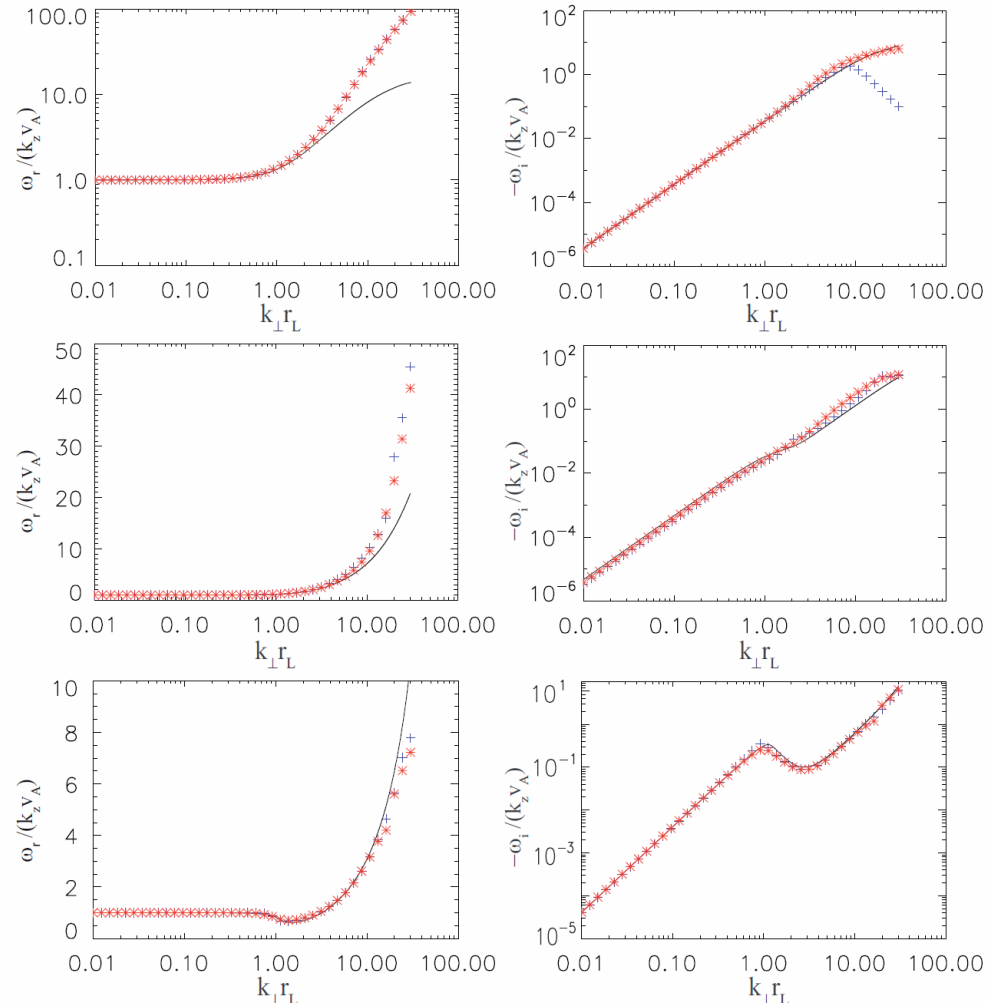
with

$$\tilde{r}_{\parallel\perp p} = -\frac{\bar{p}_{\perp p}}{2} v_{\text{th}\parallel r}^2 \left[\frac{T'_{\perp p}}{\bar{T}_{\perp p}} - \frac{1}{\Omega_p} \mathbf{b} \cdot (\nabla \wedge \mathbf{u}_p) + \left(\frac{\bar{T}_{\perp p}}{\bar{T}_{\parallel p}} - 1 \right) \frac{|\mathbf{B}|}{B_0} \right]$$

or, possibly, at the next order...

These closures provide a satisfactory model for scales up to $k_{\perp} r_L \approx 10$
when temperature anisotropy is not too large.

Frequency and damping rate of
a kinetic Alfvén wave
propagating in a direction
making an angle $\theta = 89.94^\circ$,
versus $k_{\perp} r_L$, for equal and
isotropic ion and electron
temperatures, and $\beta = 0.1$ (top),
1 (middle), 10 (bottom).



A more direct approach directly using kinetic theory and also valid at small scales

To preserve local rotational invariance one is led to write:

$$\nabla \cdot \Pi = \nabla \cdot [-\mathcal{A} \mathbf{n} + \mathcal{B} \boldsymbol{\epsilon} \cdot \mathbf{b} + \mathbf{b} \otimes \Pi_{\parallel} + \Pi_{\parallel} \otimes \mathbf{b}],$$

$$\begin{aligned} \mathcal{A} &= \bar{p}_{\perp p} \left[\frac{1}{\Omega_p} \widehat{\mathfrak{A}}_1 \mathbf{b} \cdot (\nabla \wedge \mathbf{u}_p) + \widehat{\mathfrak{A}}_2 \frac{T_{\perp p}}{\bar{T}_{\perp p}} \right] \\ \text{with } \mathcal{B} &= \frac{\bar{p}_{\perp p}}{\Omega_p} \left[\widehat{\mathfrak{B}}_3 \mathbf{n} : \nabla \mathbf{u}_p - \widehat{\mathfrak{B}}_1 \mathbf{b} \cdot \left(\nabla \wedge \frac{c \mathbf{E}_H}{B_0} \right) \right]. \end{aligned}$$

functions of transverse wavenumbers involving modified Bessel functions

with

$$\text{and } \Pi_{\parallel} = \frac{1}{\Omega_p} (2\bar{p}_{\parallel p} - \bar{p}_{\perp p}) \left(\mathbf{b} \wedge \partial_{\parallel} \mathbf{u} + \mathbf{n} \cdot \partial_{\parallel} \frac{c \mathbf{E}_H}{B_0} \right) - \mathbf{n} \cdot \nabla \mathcal{C}_2 - \mathbf{b} \wedge \nabla \mathcal{D}_2,$$

$$\mathcal{C}_2 = \frac{\bar{T}_{\perp p}}{m_p \Omega_p^2} (\bar{p}_{\perp p} - \bar{p}_{\parallel p}) \widehat{\mathfrak{C}}_3 \partial_{\parallel} \frac{|\mathbf{B}|}{B_0} + \frac{\bar{p}_{\parallel p}}{\Omega_p} \widehat{\mathfrak{C}}_2 \left(\frac{c \mathbf{E}_H}{B_0} \cdot \mathbf{b} \right)$$

with

$$-\frac{\bar{T}_{\perp p}}{m_p \Omega_p^3} (\bar{p}_{\perp p} - 2\bar{p}_{\parallel p}) \widehat{\mathfrak{C}}_4 \frac{c}{B_0} \partial_{\parallel} (\mathbf{n} : \nabla \mathbf{E})$$

One can also write:

$$\Pi_{\perp} = -[\nabla_{\perp} \otimes \nabla_{\perp} - (\mathbf{b} \wedge \nabla) \otimes (\mathbf{b} \wedge \nabla)] \Delta_{\perp}^{-1} \mathcal{A} + [\nabla_{\perp} \otimes (\mathbf{b} \wedge \nabla) + (\mathbf{b} \wedge \nabla) \otimes \nabla_{\perp}] \Delta_{\perp}^{-1} \mathcal{B},$$

A more sophisticated treatment is necessary for the D_2 term:

perpendicular pressure balance is to be imposed and q_{\perp} has to be obtained from T

One proceeds similarly, for the other tensors (heat fluxes, energy-weighted pressures,...).

- The model conserves the total energy:

$$E = \int \left[\frac{\rho|u|^2}{2} + \frac{|b|^2}{2} + \beta_{\parallel i} (p_{\perp i} + p_{\perp e} + \frac{1}{2}(p_{\parallel i} + p_{\parallel e})) \right] d\mathbf{x}$$

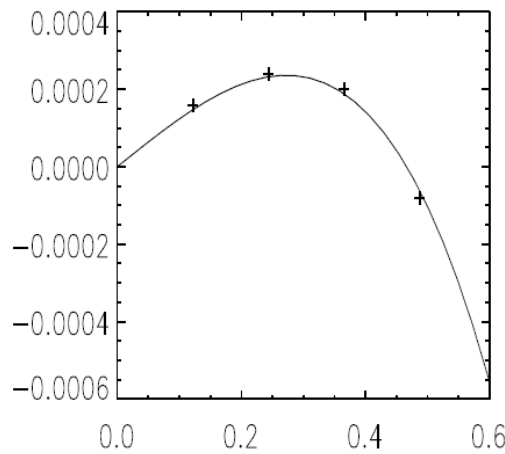
Conservation of energy is independent of the heat fluxes and subsequent equations, but requires retaining the work done by the FLR stress forces.

- Implementation of the Landau damping via Hilbert transforms, and also of the FLR coefficients as Bessel functions of $k_{\perp p}$, is easy in a spectral code.
- Electron Landau damping is an essential ingredient in many cases (limiting the range of validity of isothermal electrons often used in hybrid simulations).
- All linearized fluid equations are satisfied when plugging the fluid moments directly calculated from the LF kinetic theory, except the perpendicular velocity equation: it reduces to the perpendicular pressure balance condition, as in gyrokinetics.

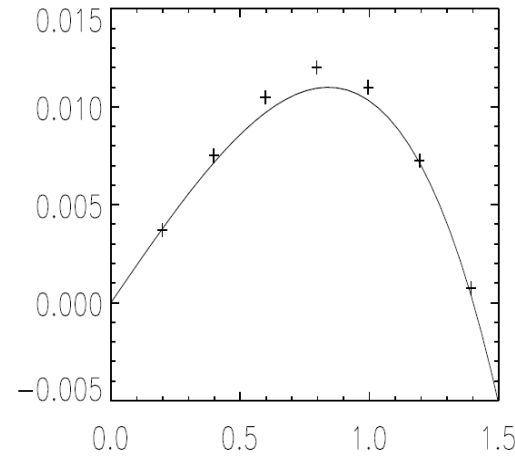
Dispersion relation of low frequency modes: comparison with linear kinetic theory

Mirror modes:

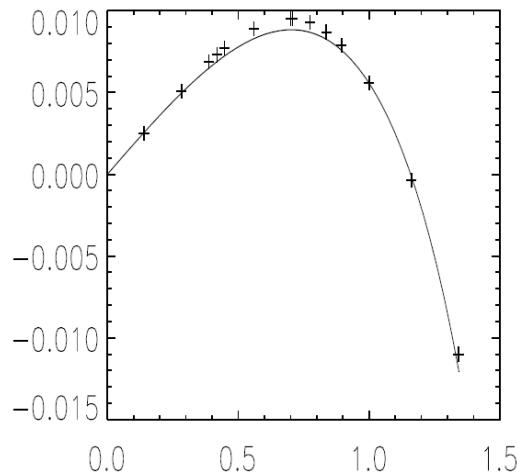
Normalized growth rate ω_i/Ω_p versus $k_\perp r_L$



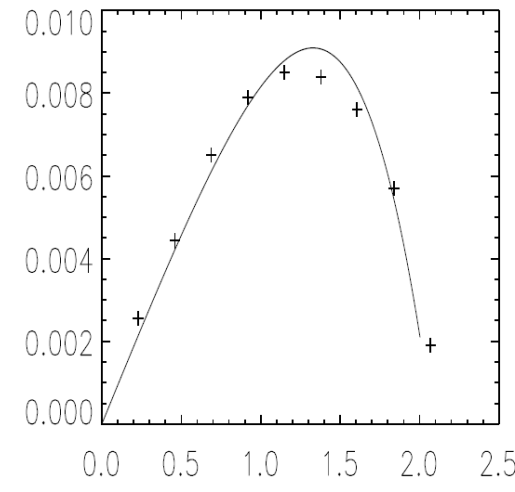
$\beta = 5$, $\tau = 0.1$, $\theta = \cos^{-1}(0.1)$,
 $T_{\perp p}/T_{\parallel p} = 1.2$ and $T_{\perp e}/T_{\parallel e} = 1$.



$\beta = 2$, $\tau = 1$, $\theta = \cos^{-1}(0.1)$,
 $T_{\perp p}/T_{\parallel p} = 2$ and $T_{\perp e}/T_{\parallel e} = 1$.



$\beta = 5$, $\tau = 1$, $\theta = \cos^{-1}(0.2)$,
 $T_{\perp p}/T_{\parallel p} = 1.4$ and $T_{\perp e}/T_{\parallel e} = 1$.



$\beta = 5$, $\tau = 1$, $\theta = \cos^{-1}(0.2)$,
 $T_{\perp p}/T_{\parallel p} = 1.1$ and $T_{\perp e}/T_{\parallel e} = 1.18$

$$\tau = T_{\parallel e}/T_{\parallel p}$$

Frequency and damping rate of Alfvén waves:

quasi-transverse propagation (Kinetic Alfvén waves)

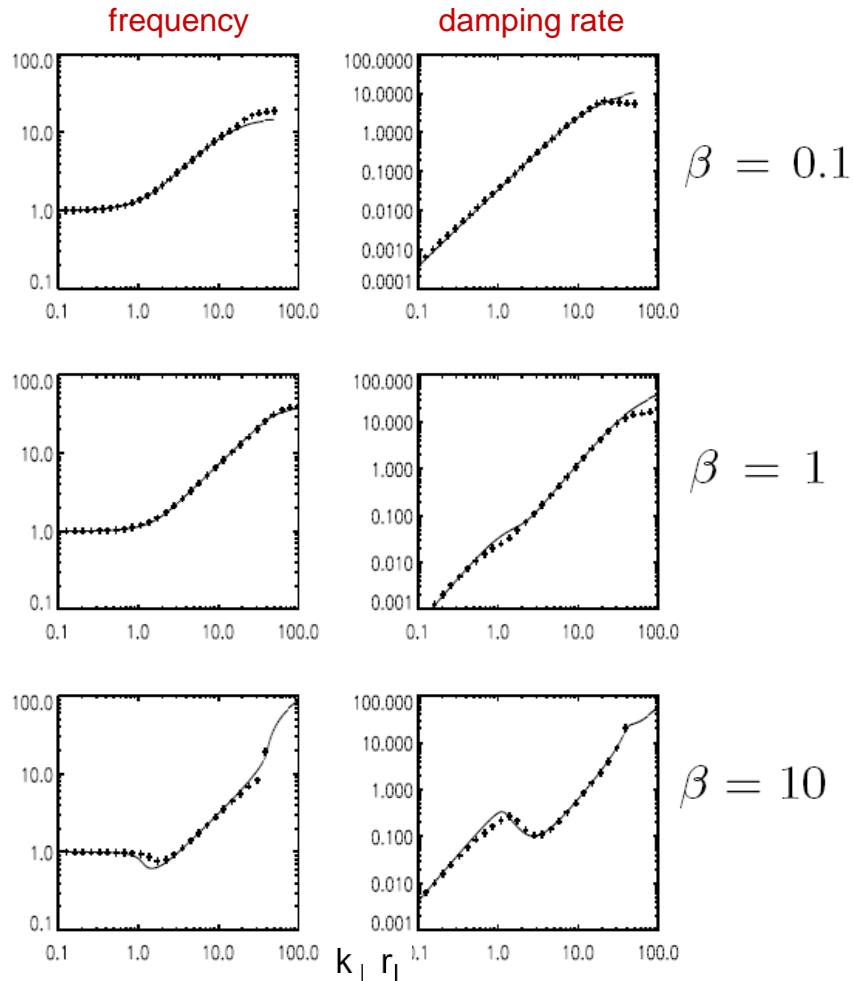


FIG. 2: Normalized frequency $\omega_r/(k_{\parallel}v_A)$ (left) and damping rate $-\omega_i/(k_{\parallel}v_A)$ (right) for KAWs with $\theta = \tan^{-1}(1000)$, $\tau = 1$, versus $k_{\perp}r_L$ for $\beta = 0.1$ (top), $\beta = 1$ (middle), $\beta = 10$ (bottom).

$\Theta=89.9^\circ$

Does not capture resonance¹

oblique propagation

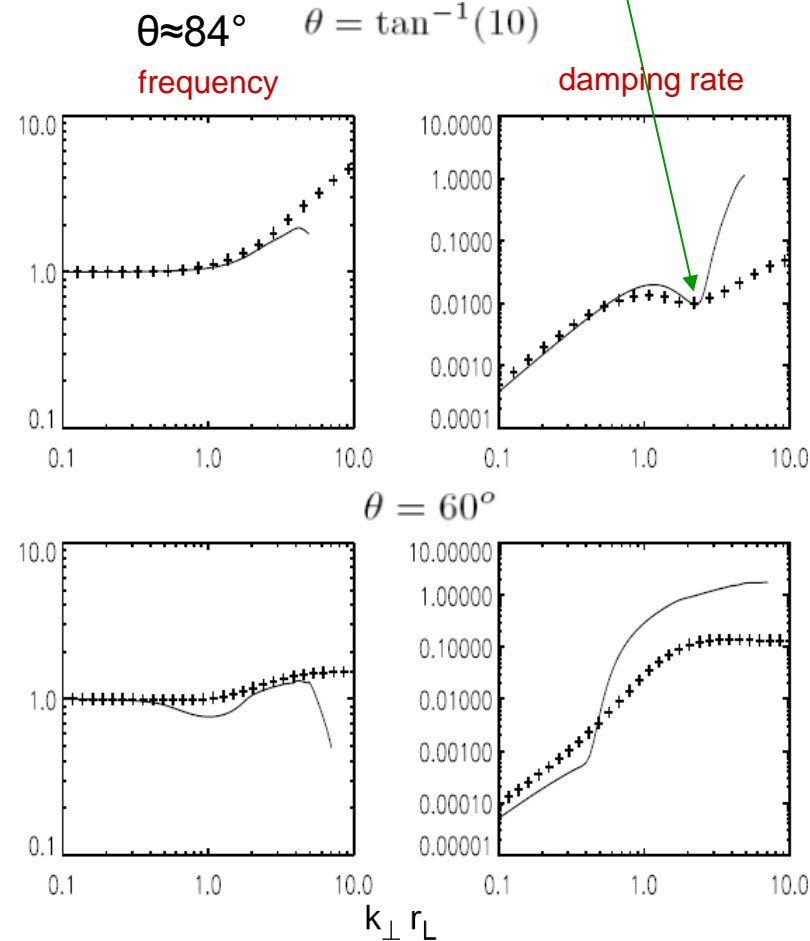
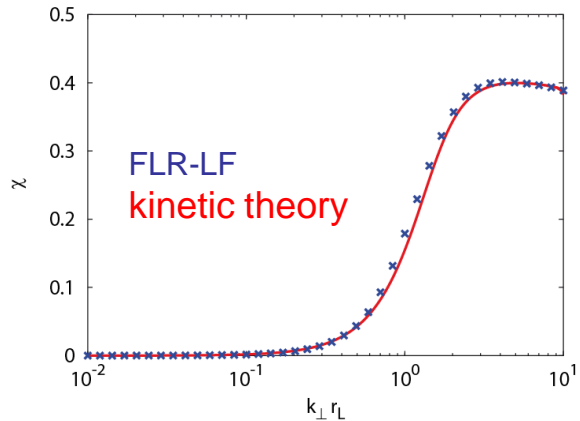


FIG. 3: Normalized frequency $\omega_r/(k_{\parallel}v_A)$ (left) and damping rate $-\omega_i/(k_{\parallel}v_A)$ (right) for KAWs with $\tau = 0.01$, $\beta = 1$ versus $k_{\perp}r_L$ for $\theta = \tan^{-1}(10)$ (top), $\theta = 60^\circ$ (bottom).

¹ : the model also captures fast waves but only up to scales where resonance appears.

Kinetic Alfvén waves eigenvectors



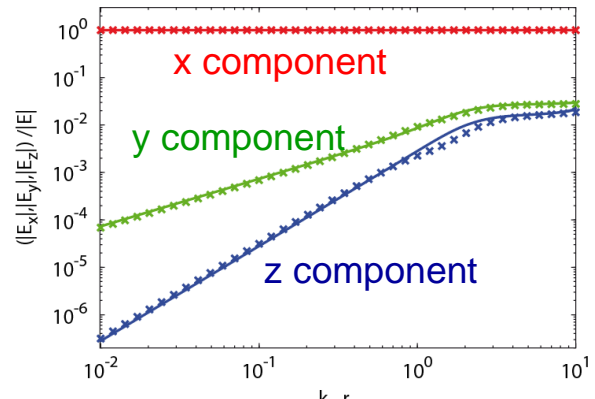
Magnetic compressibility

$$\chi = |b_z|^2 / |B|^2$$

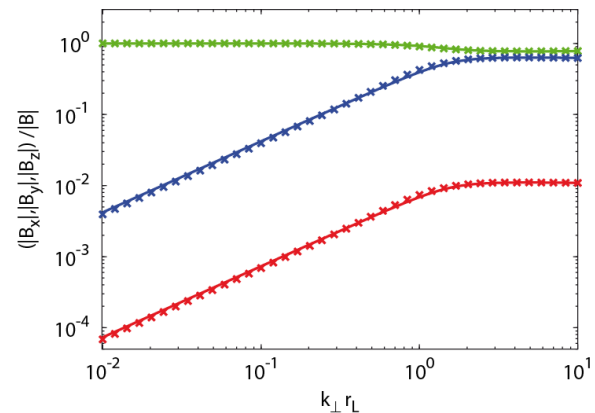
KAW, $\theta=89^\circ$

$$\begin{aligned} \beta_{\parallel} &= 2 \\ a_p = a_e &= 1 \\ T &= 1 \end{aligned}$$

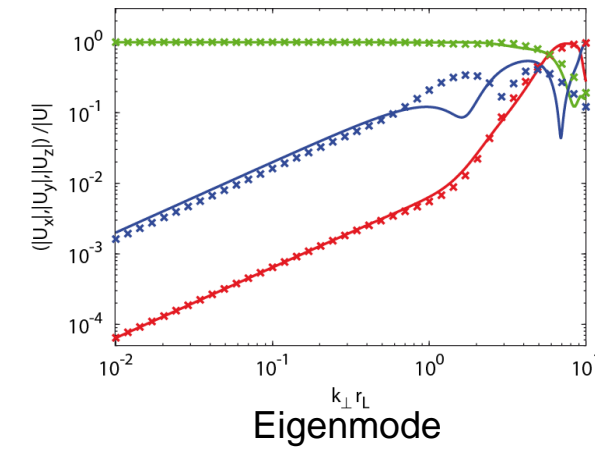
electric
field



magnetic
field



velocity
field



Comparison FLR-Landau fluid with full kinetics

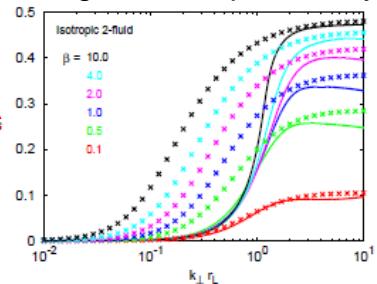
magnetic compressibility: $\chi(k_{\perp}r_L) = |B_z(k_{\perp}r_L)|^2/|B(k_{\perp}r_L)|^2$

electric field polarization: $\mathcal{P} = \text{Arg}(E_y/E_x)/\pi$.

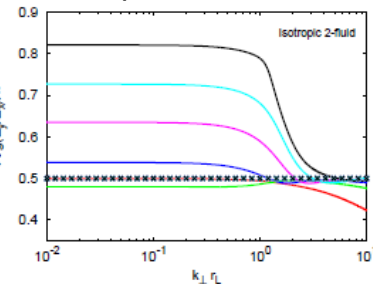
$\begin{cases} \mathcal{P} < 0 & \text{left polarized wave} \\ \mathcal{P} > 0 & \text{right polarized wave} \end{cases}$

propagation angle $\theta = 89.99^\circ$

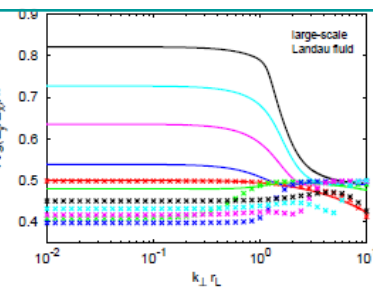
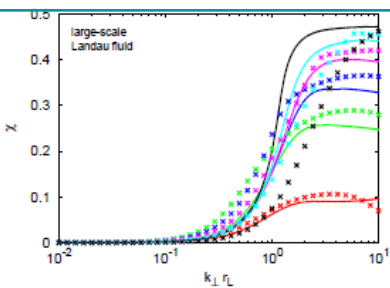
magnetic compressibility



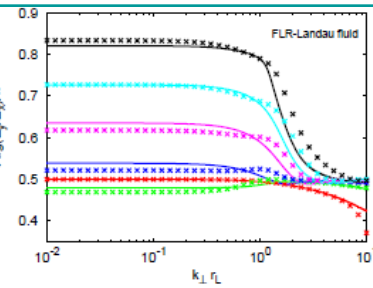
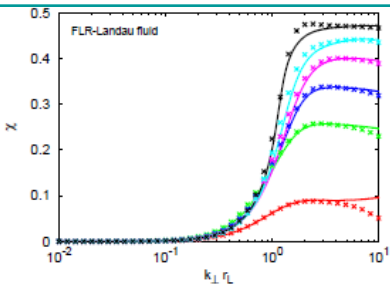
polarization



polytropic bi-fluid



LS-LF



FLR-LF

Polytropic bi-fluid : incorrect even at large scales; Landau damping is not sufficient to reproduce kinetic theory.

FLR-Landau fluid provides a precise agreement with kinetic theory
(Hunana et al. ApJ 766:93, 2013).

Anisotropy of pressure fluctuations alone introduce a major change in wave properties!

Proton beta is 0.1, 0.5, 1, 2, 4, 10

Validation in the weakly nonlinear regime

Rather rigorous fluid models can be derived from the gyrokinetic equation.

Few contain enough ingredients for $\beta \approx 1$ (e.g. allow for B_{\parallel} fluctuations)

One example is the one by Brizard : PoF 4, 1213 (1992).

Despite some shortcomings this model constitutes an interesting starting point to derive limiting equations valid for scales large compared with the electron Larmor radius and small compared with the ion Larmor radius.

Interestingly the same equations can be derived from the FLR-Landau fluid model in the weakly nonlinear limit, assuming an equilibrium state with isotropic temperature.

This provides a way of validating the semi-phenomenological character of FLR-LF models.

At small scales:

gyroaveraging (or cancellations of fluid quantities with FLR corrections in the FLR-LF model)

→ Ion velocities and ion temperature fluctuations become subdominant at small scales

Decay simulations in 3D: Reduction of compressibility and parallel transfer by Landau damping

P. Hunana, D. Laveder, T. Passot, P.L. Sulem, D. Borgogno, ApJ **743**:128 (2011)

3D MS-Landau fluid simulations in a turbulent regime

(simplified model) (*Hunana, Laveder, Passot, Sulem & Borgogno, ApJ 743, 128, 2011*).

Freely decaying turbulence (temperatures remain close to their initial values)

- Isothermal electrons
- Initially:
 - no temperature anisotropy;
 - equal ion and electron temperatures
 - incompressible velocity.

Pseudo-spectral code

Resolution: 128^3 (with small scale filtering)

Size of the computational domain: 32π inertial lengths in each direction

Initially, energy on the first 4 velocity and magnetic Fourier modes $kd_i = m/16$ ($m=1, \dots, 4$)

with flat spectra and random phase.

Comparison of MS-Landau fluids and Hall-MHD simulations

Compressibility reduction by Landau damping

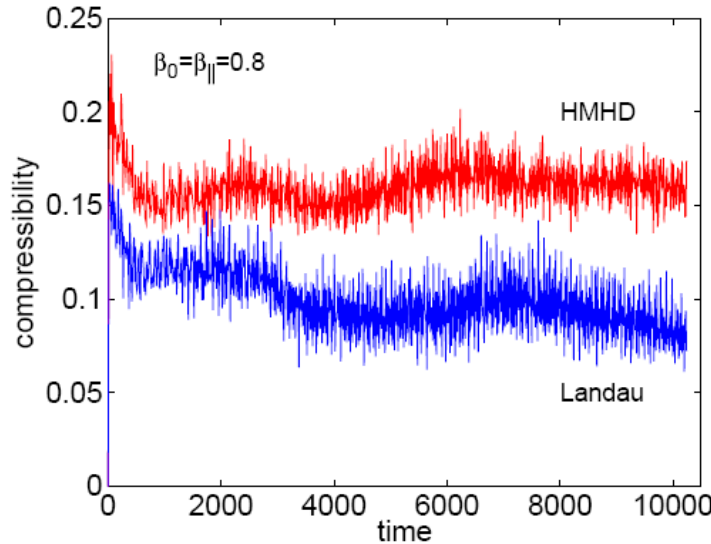
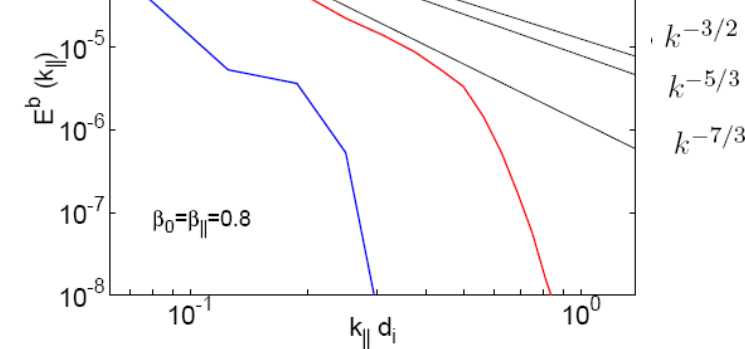
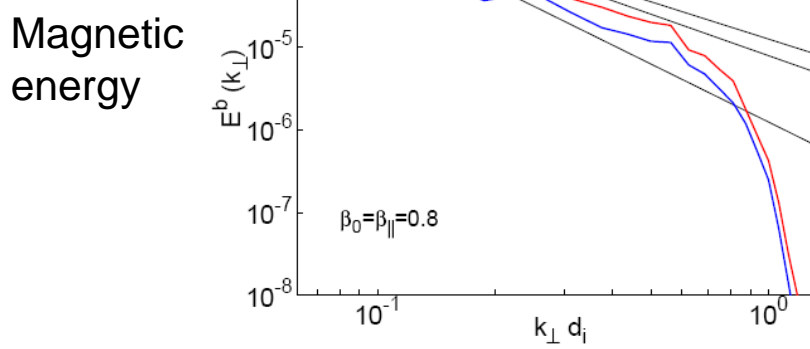
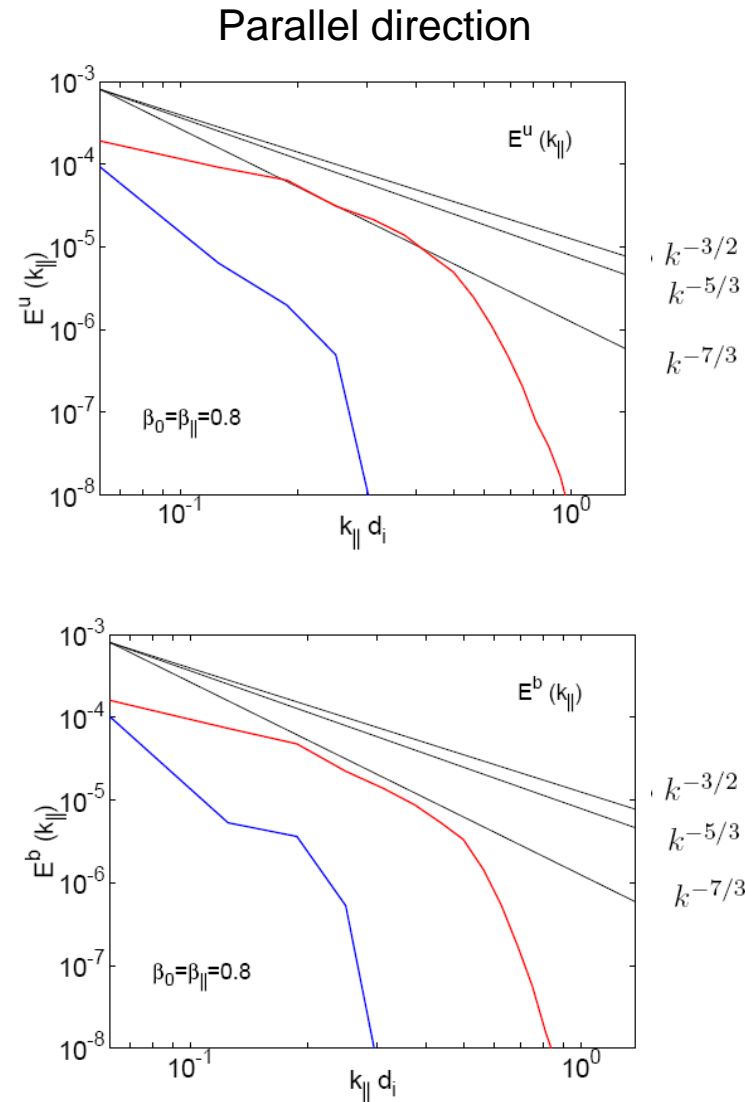
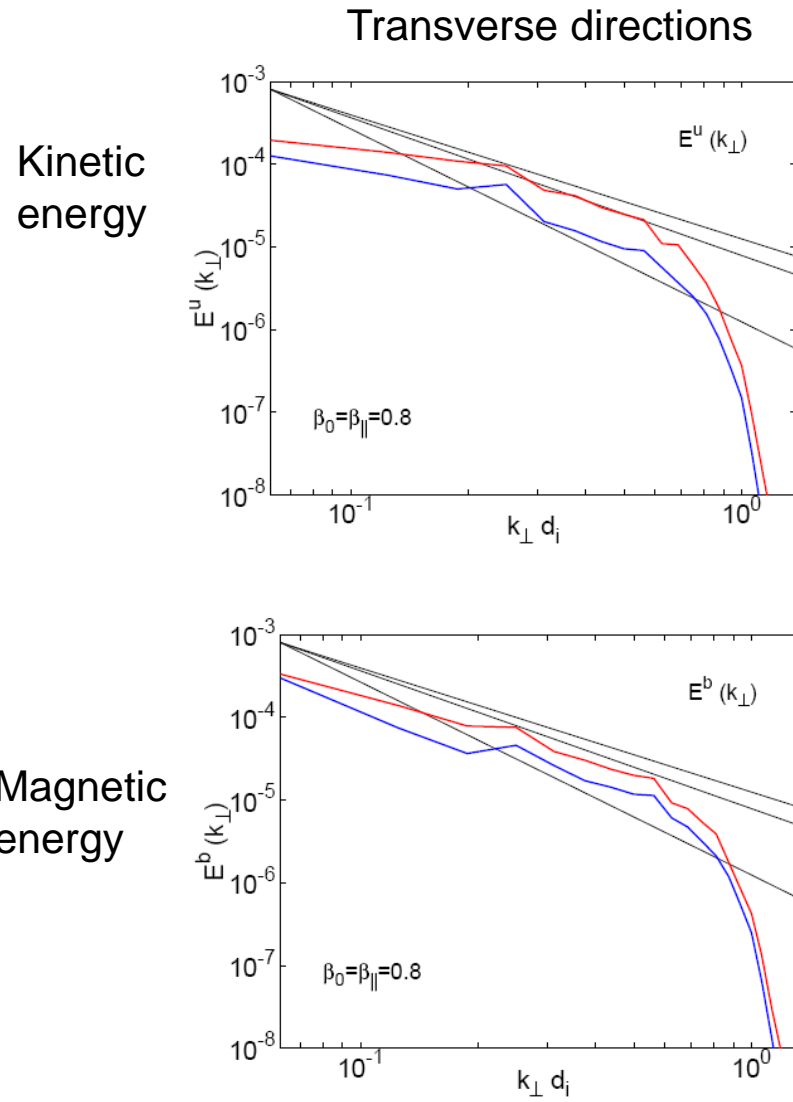


FIG. 6: Compressibility for Hall-MHD (red line) and FLR-Landau fluid (blue line) evaluated as $(\sum_k |\mathbf{k} \cdot \mathbf{u}_k|^2 / |\mathbf{k}|^2) / \sum_k |\mathbf{u}_k|^2$ for $\beta_0 = \beta_{\parallel} = 0.8$. Both regimes start with the identical initial condition where the velocity field is divergence free. The figure shows that the compressibility is clearly inhibited in the Landau fluid simulation.

Important in solar wind context: Although solar wind is a fully compressible medium, the turbulent fluctuations behave as if there were weakly compressible.

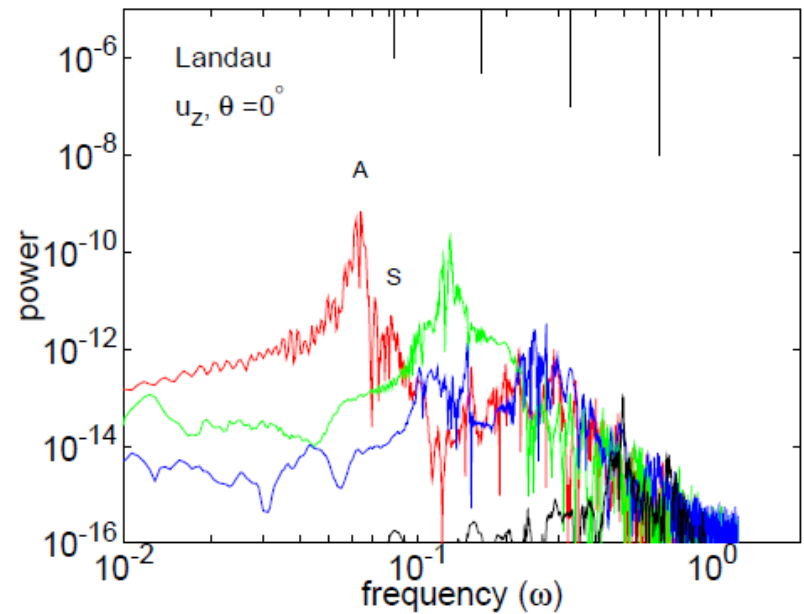
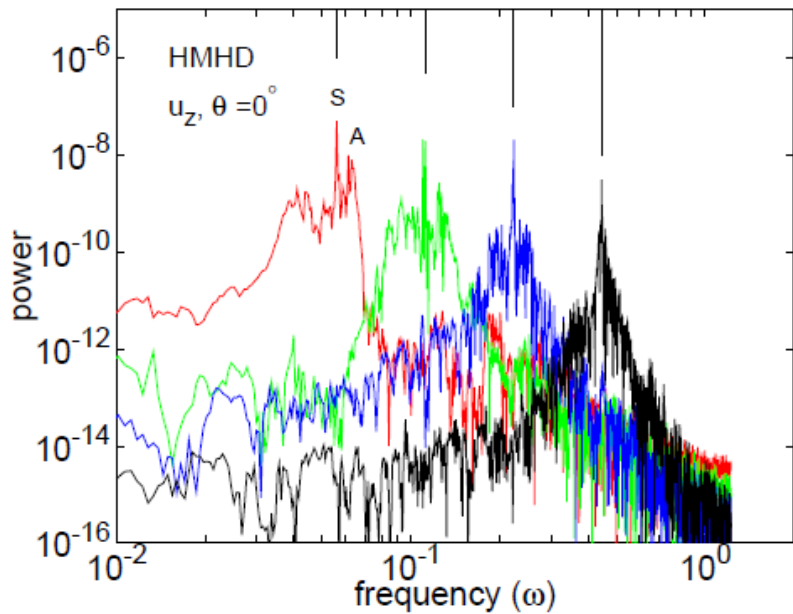
Spectral anisotropy

— Hall-MHD
— FLR-Landau fluid



Strong reduction of the parallel transfer

Damping of slow modes



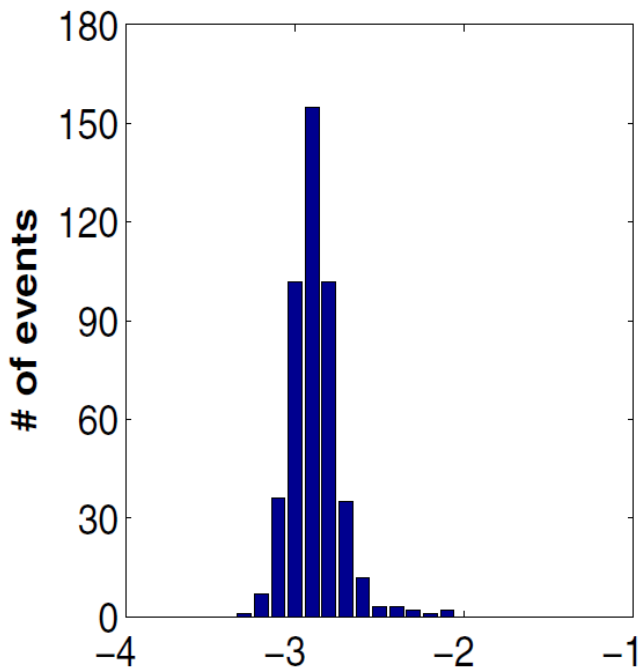
Strong damping of sound waves in oblique directions as well,
but not in the perpendicular one.

Non-universality at sub-ion scales

Spectral exponent at sub-ion scales, excluding the transition range

Magnetic spectrum in the solar wind

(Cluster observations)



Sahraoui et al., ApJ **777**, 15, 2013

“the slopes of the spectra in the dispersive range (i.e., $[f_{\rho_i}, f_{\rho_e}]$) cover the domain $\sim [-2.5, -3.1]$ with a peak at ~ -2.8 ”, while inertial range slopes: -1.63 ± 0.14 (Smith et al. ApJ **645** L85 (2006) using ACE)

3D Electron-MHD in the presence of a strong magnetic field

(Meyrand & Galtier, PRL **111**, 264501, 2013)

Existence of a $k_{\perp}^{-8/3}$ spectral range

2D simulations in the plane perpendicular to the ambient field

Hybrid-PIC (Franci et al., ApJL.. **804**, L39, 2015)

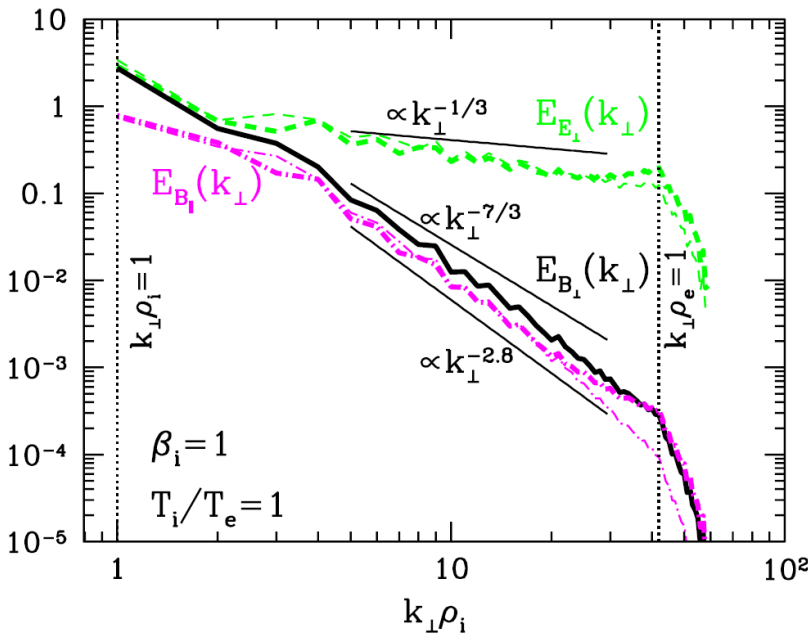
-5/3 spectrum at the MHD scales

-3 spectrum at the sub-ion scales

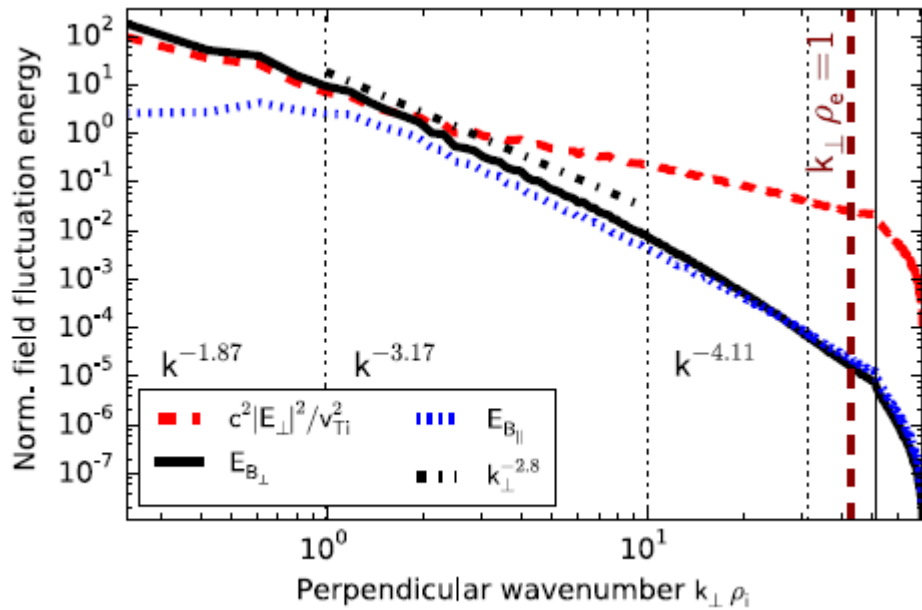
Hybrid-eulerian (Cerri et al. ApJL 2016)

B slope in sub-ion range
between -8/3 and -3

Gyrokinetic simulations



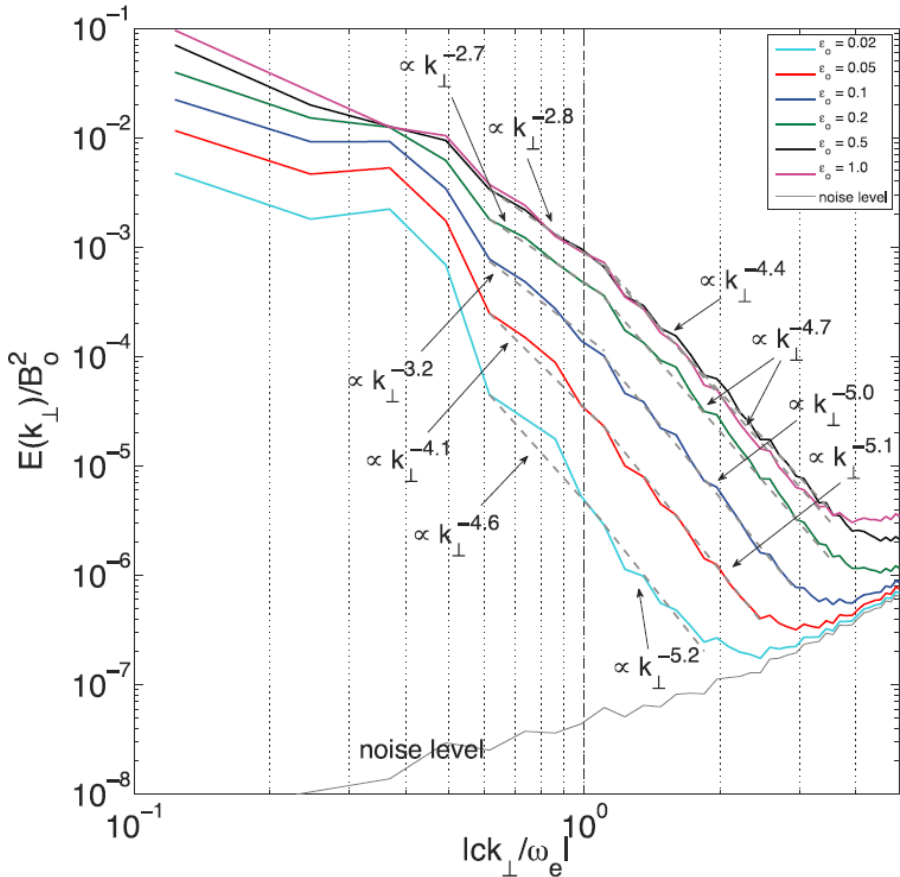
(Howes et al., PRL **107**, 035004, 2011)



(Told et al., PRL **115**, 025003, 2015)

3D full PIC whistler mode simulations

with various level of energy fluctuations (Gary et al., ApJ 755, 142, 2012)



“Increasing initial fluctuation amplitudes over $0.02 < \epsilon_0 < 0.50$ yields ... a **consistent decrease in the slope of the spectrum** at $k_{\perp} c/\omega_e < 1$ ”.

In apparent contrast to solar wind observations of Smith et al. (2006), Bruno et al. ApJL (2014). (several parameters probably simultaneously changed and/or problem with definition of fluctuation amplitude)

Main points to understand, focusing on sub-ion spectral slopes

1. The observed spectra are **steeper than the -7/3 slope** predicted by most theories based on critical balance arguments.
2. Except in simpler models, the slopes display a rather **large scatter**.

Questions:

- What is the **correlation between the spectral slopes** and:
 - the **amplitude** of magnetic field fluctuations
(to be defined properly)
 - the strength or **transfer rate of the turbulence**
(as e.g. defined by extensions of Karman-Howarth equation
as in Banerjee & Galtier PRE **87**, 013019 (2013))
 - the **beta** parameter

Reduced models

Need to perform large-scale simulations aiming at testing theories.

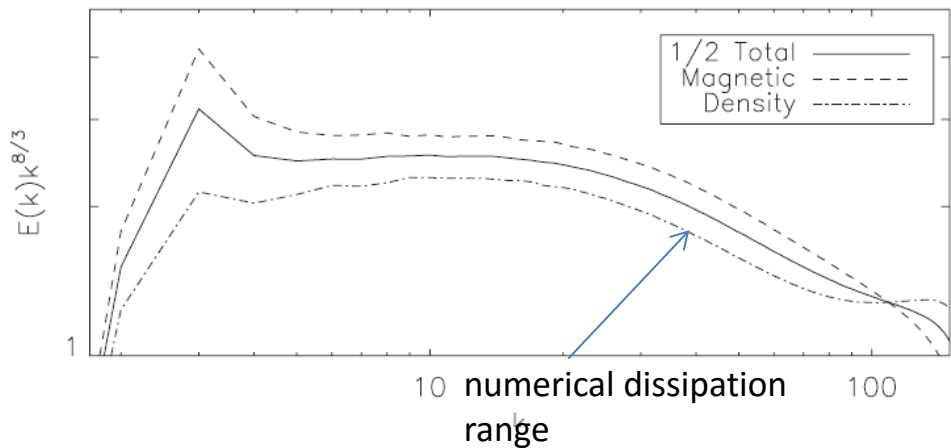
Such simulations have been done using a semi-phenomenological model assuming Boltzmannian ions and electrons:

Boldyrev & Perez, ApJL, **758**, L44, 2012; see also Schekochihin et al. ApJ Supp. **182**, 310 (2009)

$$\begin{aligned}\partial_t \psi + \nabla_{\parallel} n &= 0, & \nabla_{\parallel} &= \nabla_z + \hat{z} \times \nabla \psi \cdot \nabla_{\perp} \\ \partial_t n - \nabla_{\parallel} \nabla_{\perp}^2 \psi &= 0 & \mathbf{b}_{\perp} &= \hat{z} \times \nabla \psi\end{aligned}$$

$E = \int (|\nabla \psi|^2 + n^2) d^3x$ is conserved.

Power counting gives exponent $-7/3$
but numerics suggests $-8/3 \approx 2.7$
(viewed as intermittency corrections)



Spectrum independent of simulation parameters

Influence of Landau damping

(Howes et al. *JGR* 113, A05105, 2008; *PoP* 18, 102305, 2011):

Balance between energy transfer and Landau dissipation:

leads essentially to energy flux $\epsilon \sim \exp(-\lambda k_{\perp})$ and $E(k_{\perp}) \sim k_{\perp}^{-7/3} \exp(-2\lambda k_{\perp}/3)$

For appropriate parameters gives the impression of a steeper power law.

Revised version (*Passot & Sulem Ap.J. Lett.* 812: L37, 2015) predicts a **non-universal correction to the power-law exponent**.

Need to include both ion and electron Landau damping

→ Turn to the **FLR-Landau fluid model** to perform runs with varying parameters

Alfvenic turbulence

The system is driven by a random forcing

$$F_i(t, \mathbf{x}) = \sum_{1 < n < N} F_{i,n}^0 \cos(\omega_{KAW}(\mathbf{k}_n)t - \mathbf{k}_n \cdot \mathbf{x} + \phi_{i,n})$$

KAWs are generated by resonance

KAW frequency of wavevector \mathbf{k}_n
Propagation angle : $80^\circ - 86^\circ$

Driving is turned on (resp. off) when the sum of kinetic and magnetic energies is below (resp. above) a prescribed threshold: **prescribed amplitude of the turbulence fluctuations.**

Initially, equal isotropic ion and electron temperatures with $\beta_i = \beta_e = 1$

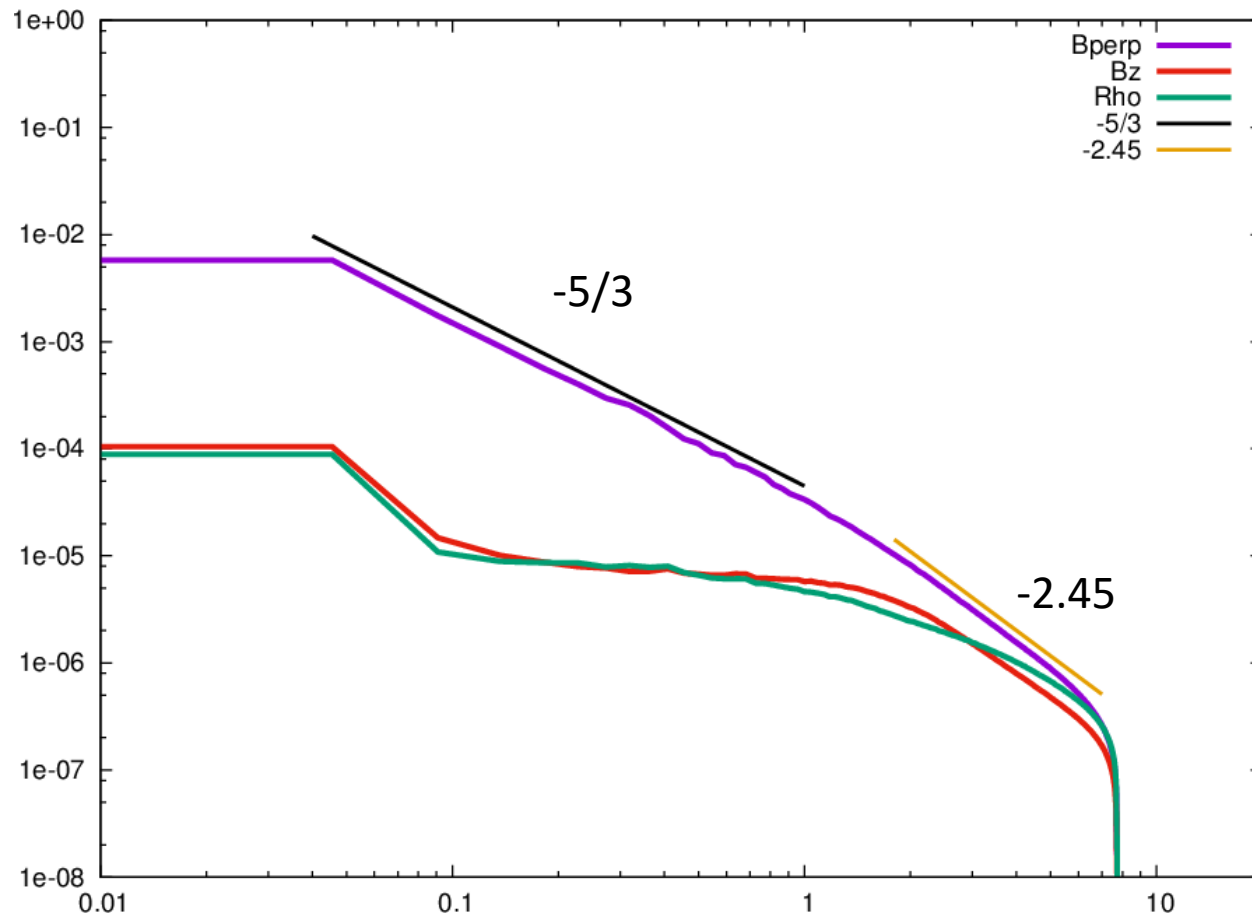
Use of a Fourier spectral method in a 3D periodic domain, 5.7 to 14 times more extended in the parallel direction than in the perpendicular ones.

Realistic mass ratio → sub-stepping of temporal scheme for electron temperature/heat flux equations.

Weak hyperviscosity and hyperdiffusivity (k^8 operator) are supplemented

- to ensure the presence of a numerical dissipation range,
- to mimic the effect of Landau dissipation at ion scales not retained in the simulation (do not affect spectral exponents).

Resolution of 128^3 (up to $512^2 \times 256$) points before aliasing is removed.



Simulation at $\beta=1$ including a Kolmogorov range.
Clear spectral break near $k_{\perp}r_L=1$

Flat density and B_z spectra at large scales that tend to asymptote the B_{\perp} spectrum in the sub-ion range.

Simulations concentrating on the sub-ion range, performed for various amplitudes of turbulent Alfvénic fluctuations, and various propagation angles.

	Run A+	Run A	Run B80	Run B83	Run B86
Angle of injected KAWs	80°	80°	80°	83.6°	86°
rms of v_{\perp} and B_{\perp}	0.2	0.13	0.08	0.08	0.08
L_{\perp}/L_{\parallel}	0.18	0.18	0.18	0.11	0.07
rms of resulting density fluctuations	0.045	0.03	0.014	0.016	0.017
Transverse magnetic spectrum exponent	-2.3	-2.6	-3.6	-2.8	-2.3
$A = (k_z/k_0)(B_0/\delta B_{\perp 0})$	0.9	1.4	2.2	1.4	0.9

KAW modes driven at $|k d_i| = 0.18$ (the largest scales), and propagation angles with the ambient field of 80° , 83.6° and 86° (varied by changing the parallel size of the domain).

A main result: the dynamics is strongly sensitive to the **nonlinearity parameter**

$$\chi = \omega_{NL}/\omega_W$$

ratio of the nonlinear frequency (of the transverse dynamics) to the kinetic Alfvén wave frequency (along the magnetic field lines)

$$\omega_{NL} = \sqrt{k_{\perp}^5 E(k_{\perp})} \quad (\text{constructed from electron velocity})$$

$$\omega_W = \bar{\omega}(k_{\perp} \rho_i) v_A k_{\parallel}$$

$$\bar{\omega}(k_{\perp} \rho_i) \quad \text{given by linear kinetic theory}$$

k_{\parallel} : wavenumber along the magnetic field lines
(to be defined)

Turbulence anisotropy

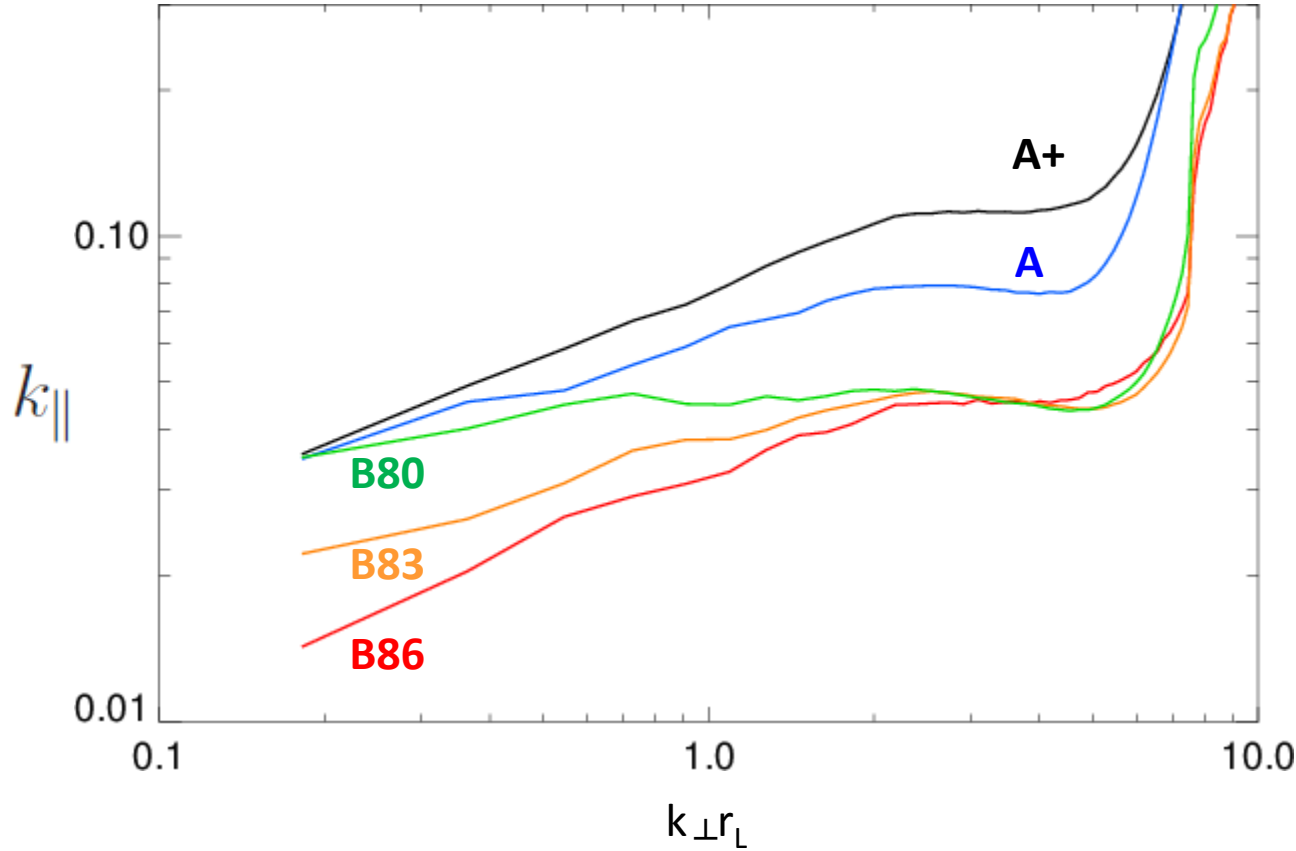
Parallel wave number along the local magnetic field line of an eddy with transverse wavenumber k_{\perp} (*Chow & Lazarian, ApJL 615, L41, 2004*)

$$k_{\parallel}(k_{\perp}) \approx \left(\frac{\sum_{k \leq |k'| < k+1} |\widehat{\mathbf{B}_L \cdot \nabla \mathbf{b}_l}|_{k'}^2}{B_L^2 \sum_{k \leq |k'| < k+1} |\widehat{\mathbf{b}}|_{k'}^2} \right)^{1/2}$$

\mathbf{B}_L is the local mean field obtained by eliminating modes whose perpendicular wavenumber is greater than $k/2$

The fluctuating field \mathbf{b}_l is obtained by eliminating modes whose perpendicular wavenumber is less than $k/2$.

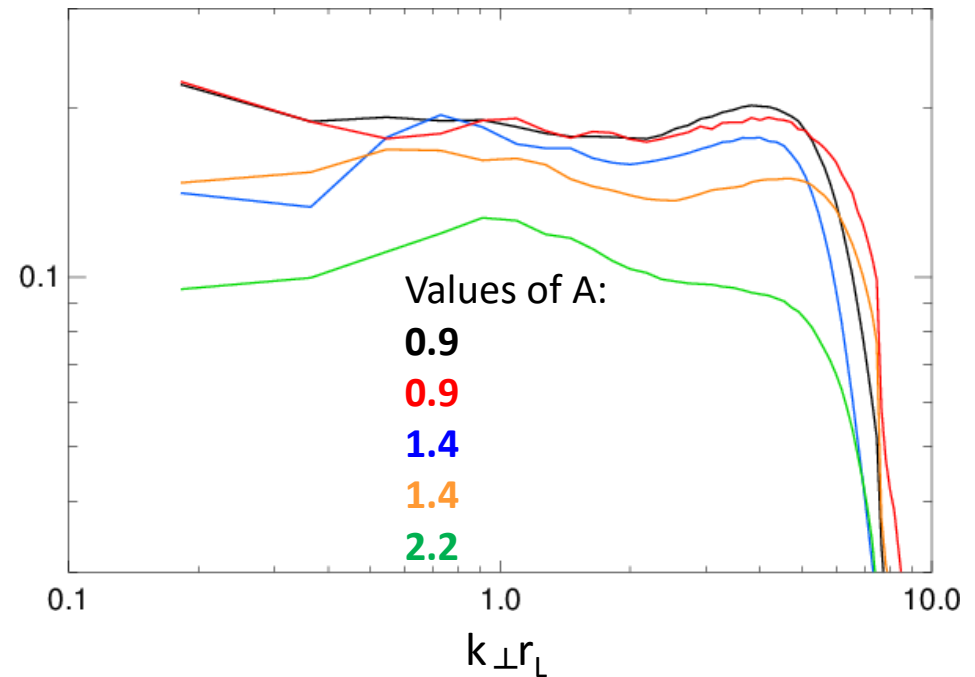
Parallel wavenumber defines the inverse correlation length **along magnetic field lines**, at a specified transverse scale.



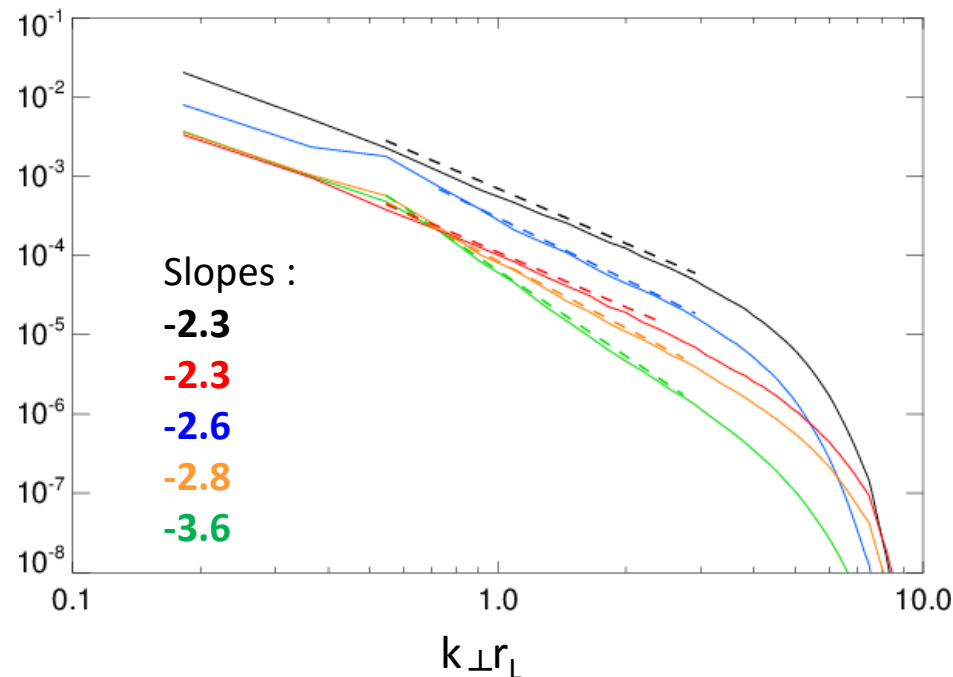
For small amplitude fluctuations, (B80), k_{\parallel} is rather flat, suggesting weak turbulence.

For larger amplitudes, k_{\parallel} grows as a power law (as expected in a strong turbulence regime), and saturates at small scales.

$$\chi = \omega_{NL}/\omega_W$$



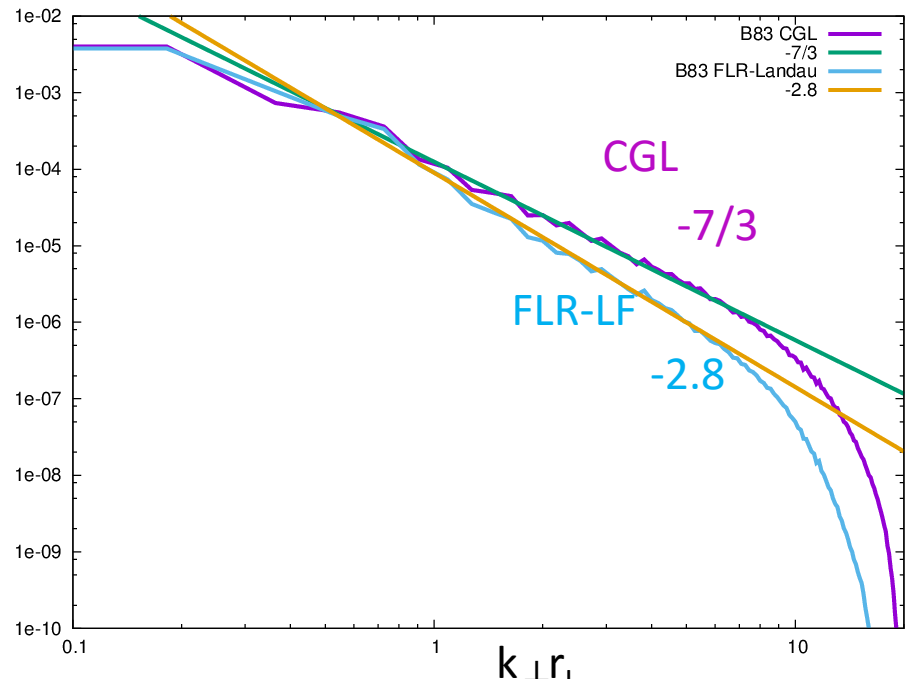
$$E_{B\perp}(k_{\perp})$$



Spectra averaged over $150 \Omega_i^{-1}$
in the quasi-stationary regime.

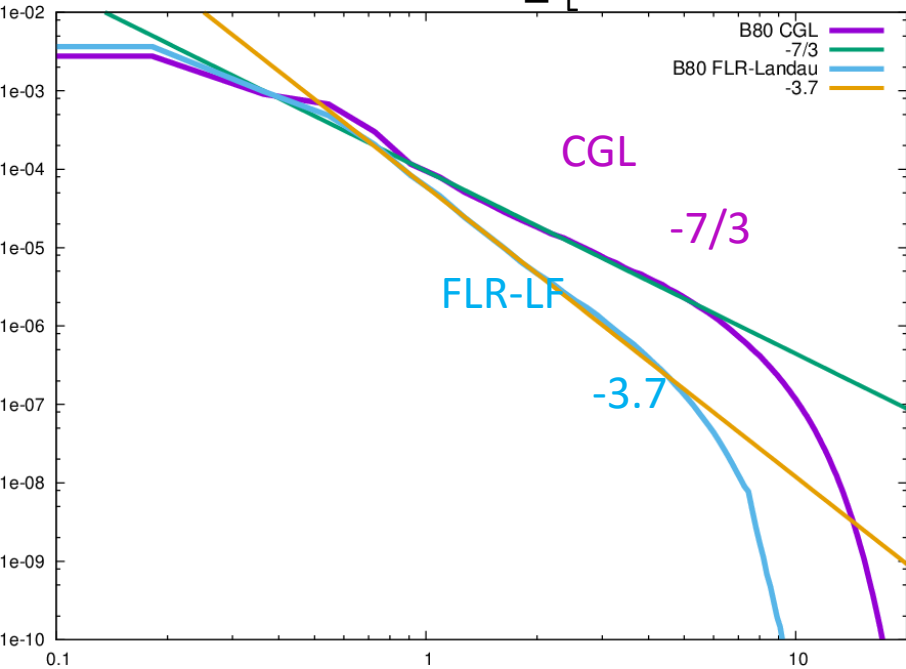
When the parameter $A = (k_z/k_0)(\delta B_{\perp 0}/B_0)^{(-1)}$ is small enough critical balance is satisfied.

Spectra are steeper when the nonlinearity parameter is smaller.



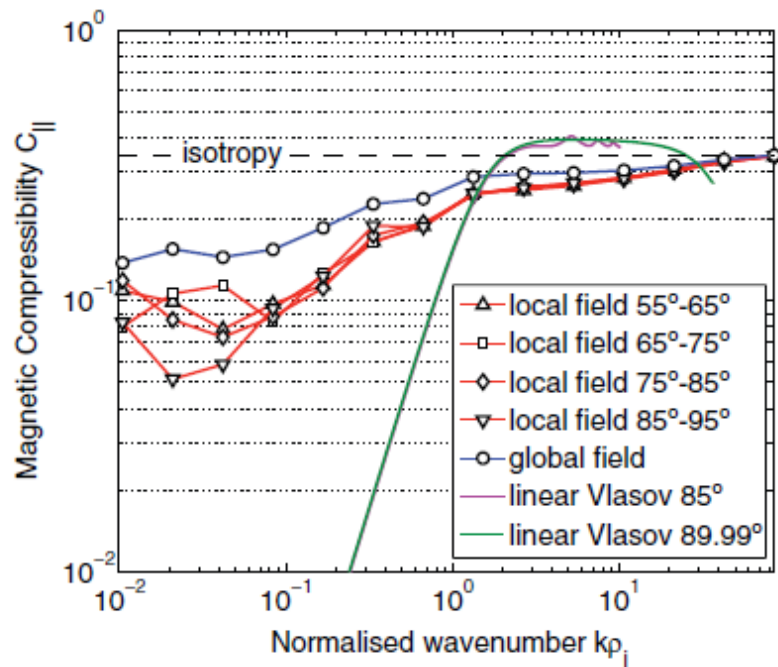
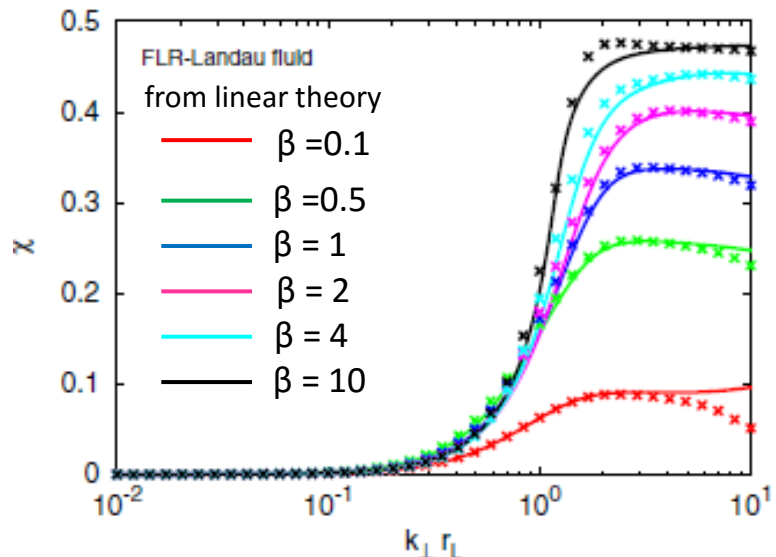
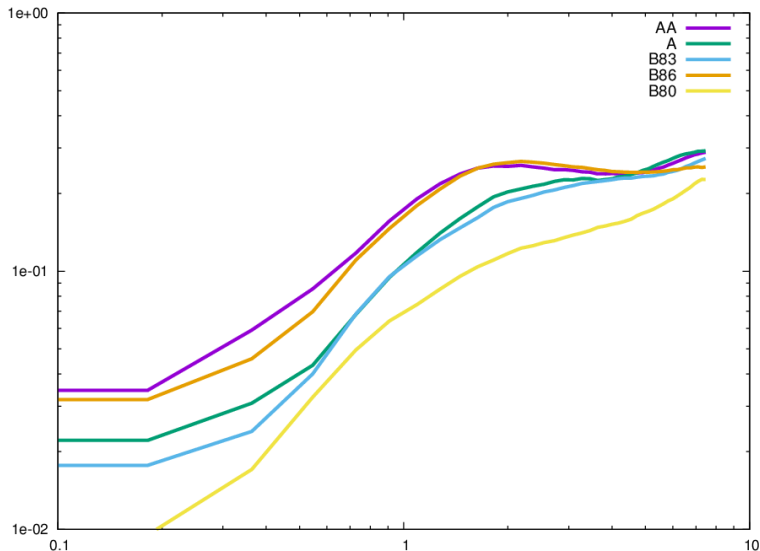
Magnetic spectra obtained with a **CGL** model with Hall effect (but **no Landau damping**), **display a $-7/3$ spectrum whatever the χ parameter**.

The slope variation results from Landau damping.



Magnetic compressibility spectrum

$$\chi(k_{\perp}r_L) = |B_z(k_{\perp}r_L)|^2 / |B(k_{\perp}r_L)|^2$$



Magnetic compressibility from Cluster data
(Kiyani et al. ApJ 763, 10, 2013)

Hunana, Golstein, Passot, Sulem, Laveder & Zank,
Astrophys. J. 766, 93 (2013); Solar Wind 13 Proceedings.

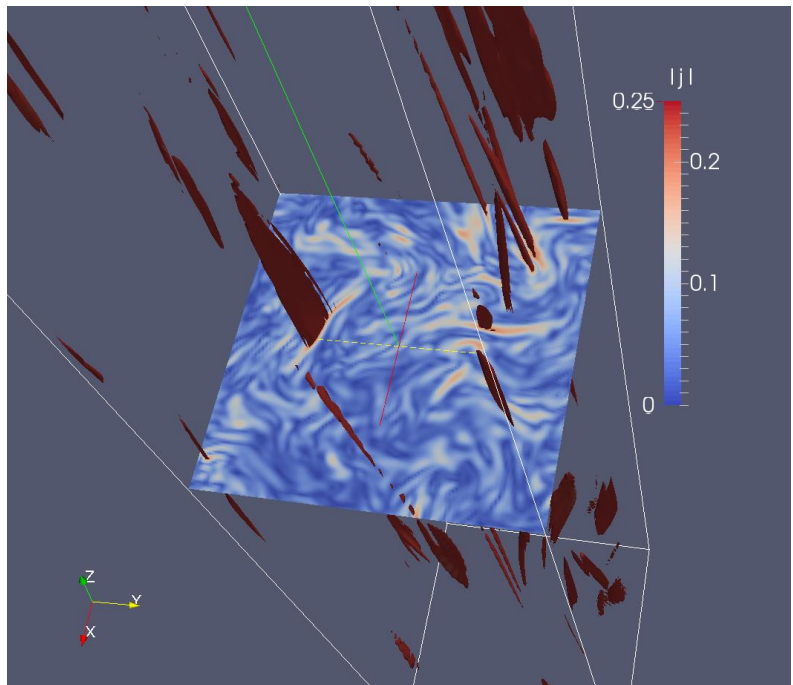
$\theta = 89.99^\circ$ (in order to accurately capture large k_{\perp})

Structures of the electric current:

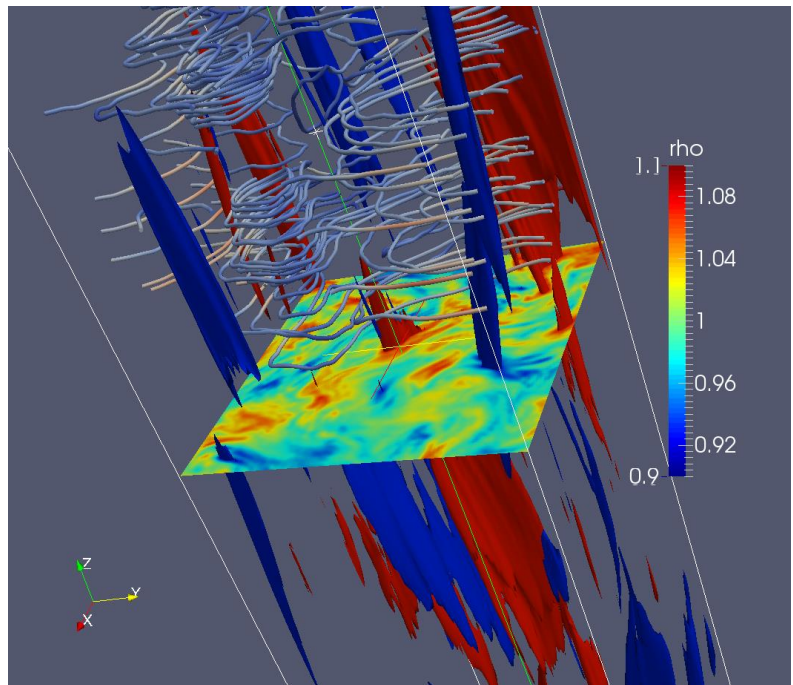
- Usual MHD leads to **current sheets**
- **Current filaments** obtained in incompressible Hall-MHD
(*Miura & Araki , J. Phys. Conf. Series 318, 072032, 2011*)
and in Electron MHD
(*Meyrand & Galtier, Phys. Rev. Lett. 111, 264501, 2013*),
due to Hall term.

Both filaments and sheets are observed.

Run A



Current



Density and ion velocity field lines

Both current sheets and filaments.

A phenomenological model for KAW turbulence

Extend analysis of Howes et al. (2008, 2011) by

- Retaining the influence on the energy transfer time, of the process of ion temperature homogenization along the magnetic field lines induced by Landau damping.
- Improving description of nonlocal interactions.

Main results:

- Critical balance establishes gradually as k_{\perp} increases, permitting a weak large-scale turbulence to become strong at small enough scales.
- Non-universal power-law spectrum for strong turbulence at the sub-ion scales with an exponent which depends on the saturation level of the nonlinearity parameter $\chi = \omega_{NL}/\omega_W$, covering a range of values consistent with solar wind and magnetosheath observations.

Stretching frequency Alfvén wave frequency

T. Passot & P.L. Sulem, *Astrophys. J. Lett.*, **812**, L37 (2015).

For the sake of simplicity , concentrate on the case where nonlinear interactions are local, i.e. energy spectrum not too steep, which is the case for $\beta \approx 1$.

More general case addressed in *Passot & Sulem (ApJL, 2015)*

Involved frequencies:

Nonlinear frequency: $\omega_{NL} = \Lambda (k_{\perp}^5 d_i^2 E_k)^{1/2}$ ($\omega_{NL} \sim k_{\perp} v_{ek}$, $v_{ek} = k b_k$, $b_k \sim (k_{\perp} E_k)^{1/2}$)

Λ : numerical constant of order unity ; $E_k \equiv E(k_{\perp})$

Frequency of KAWs propagating along the distorted magnetic field lines:

$\omega_W = \bar{\omega} k_{\parallel} v_A$ (where $\bar{\omega}$ scales like $k_{\perp} \rho_i$)

KAW Landau damping rate: $\gamma = \bar{\gamma} k_{\parallel} v_A$

(where $\bar{\gamma}$ scales approximately like $k_{\perp}^2 \rho_i^2$, at least for β of order unity)

Homogenization frequency (for each particle species) : $\omega_H = \mu k_{\parallel} v_{th}$

(where μ is a proportionality constant of order unity)

In the case of ions, comparable to other inverse characteristic time scales.

The corresponding frequency is much higher in the case of electrons (due to mass ratio), making electron homogenization along magnetic field lines too fast to have a significant dynamical effect.

Determination of the inverse transfer time or its inverse ω_{tr}

Proceeding as in the spirit of the two-point closures for hydrodynamic (Orszag 1970, Sulem et al. 1975, Lesieur 2008) or MHD (Pouquet 1976) homogeneous turbulence,

$$\omega_{tr} = \frac{\omega_{NL}^2}{\omega_W + \omega_H} = \frac{\Lambda^2 \bar{\alpha}^2 k_\perp^3 E_k}{\bar{\omega} v_A k_\parallel + \mu v_{th} k_\parallel}$$

where $\bar{\alpha} = \bar{\omega} \sim k_\perp \rho_i$.

Turbulence energy flux: $\epsilon = C \omega_{tr} k_\perp E_k$

where C is a negative power of the Kolmogorov constant.

It follows that

$$\epsilon = \frac{C \Lambda^2 \bar{\alpha}^2 k_\perp^4 E_k^2}{(\bar{\omega} v_A + \mu v_{th}) k_\parallel}$$

where the homogenization frequency contribution becomes negligible at scales for which $k_\perp \rho_i \gg 1$.

Assuming a critically balanced regime where $k_{\parallel} v_A = (k_{\perp}^3 E_k)^{1/2}$,

one has $\omega_{NL} = \Lambda \omega_w$

leading to identify the constant Λ with the nonlinearity parameter.

One thus gets

$$E_k \sim \Lambda^{-4/3} C^{-2/3} \epsilon^{2/3} k_{\perp}^{-7/3}.$$

Here, due to Landau damping, ϵ is a function of $k_{\perp} \rho_i$ and decays along the cascade.

Phenomenological equation for KAW's energy spectrum when retaining linear Landau damping (*Howes et al. 2008, 2011*)

Steady state,
outside the
Injection range

$$\partial_t \cancel{E}_k + \mathcal{T}_k = -2\gamma E_k + \cancel{S}_k$$

transfer Landau driving term
 damping acting at large scales

$$\mathcal{T}_k = \partial \epsilon / \partial k_{\perp}$$

In a critically balanced regime, this equation is solved as

$$\epsilon = \epsilon_0 \exp \left[-2C^{-1}\Lambda^{-2} \int_{k_0}^{k_\perp} \frac{\bar{\gamma}}{\xi \bar{\alpha}^2} (\bar{\omega} + \mu\beta^{1/2}) d\xi \right]$$

From linear kinetic theory,

$$\begin{cases} \bar{\alpha} = \bar{\omega} \\ \bar{\gamma}/\bar{\omega}^2 \approx \delta(\beta) \approx 0.78\rho_e/\rho_i \\ \bar{\omega} \approx a(\beta)k_\perp \quad \text{with } a(\beta) = (1 + \beta)^{-\frac{1}{2}}. \quad \text{when } \beta = 1 \end{cases} \longrightarrow \text{Leads to a log term}$$

This leads to $\epsilon_k \sim \epsilon_0 k_\perp^{-\zeta} \exp[-2a(\beta)C^{-2}\Lambda^{-2}\delta(\beta)k_\perp]$

with $\zeta = 2\delta(\beta)C^{-1}\mu\Lambda^{-2}\beta^{1/2}$.

Finally,

Involves proportionality constants C and μ which are to be empirically determined by prescribing for example that the exponential decay occurs at the electron scale.

$$E_k \sim k_\perp^{-(7/3+2\zeta/3)} \exp \left[-\frac{4}{3}a(\beta)\delta(\beta)C^{-1}\Lambda^{-2}(k_\perp\rho_i) \right].$$

The correction in the exponent is not universal: expected when dissipation and nonlinear transfer times display the same wavenumber dependence (Bratanov et al. PRL **111**, 075001 (2013)).

More quantitative analysis by numerical simulations of the differential system.

For example:

rate of strain: $\omega_{NL} \sim k_{\perp} v_{ek} = \Lambda \sqrt{\int_0^{k_{\perp}} \bar{\alpha}^2 p_{\perp}^2 E_p dp}$ Transverse magnetic spectrum
(by electron velocity gradients)

$$\bar{\alpha} = 1 \text{ for } k_{\perp} \rho_i \ll 1 \quad (v_{ek} \approx v_{ik})$$

rate of strain due to all the scales larger than $1/k_{\perp}$ (Elisson 1961, Panchev 1971)

$$\bar{\alpha} \sim k_{\perp} \rho \text{ for } k_{\perp} \rho_i \gg 1 \quad (v_{ek} \sim j)$$

Local expression recovered when the Integral diverges at large k_{\perp}

is replaced by:

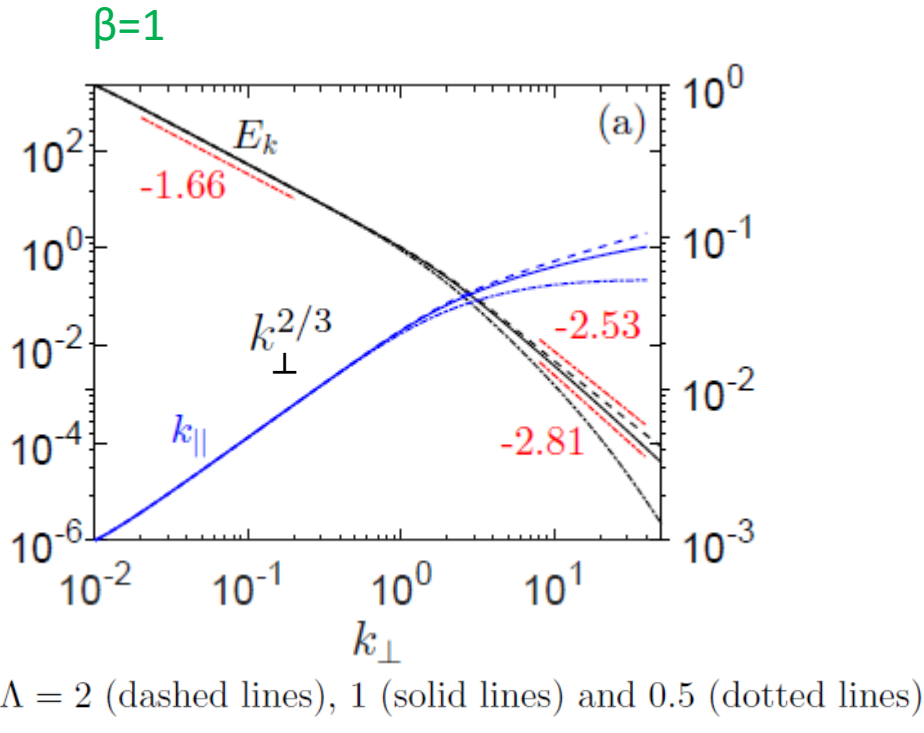
$$d\omega_{NL}^2 / dk_{\perp} = \Lambda^2 \beta^{-1} \bar{\alpha}^2 k_{\perp}^2 E_k$$

Differential system:

- Retains nonlocal interactions (relevant for relatively steep power-law spectra)
- Permits variation of the nonlinear parameter along the cascade and **transition from large-scale weak turbulence to small-scale strong turbulence**

The functions γ and ω are obtained using the WHAMP software

Phenomenological model



Range for extended sub-ion power law

Λ	0.71	1	1.22	1.30	1.41	2	4.47
exponent	-3.18	-2.81	-2.68	-2.66	-2.63	-2.53	-2.45

Sub-ion exponent depends on the saturation value Λ of the nonlinear parameter. Range of variations comparable to observations.

Solar wind observations

Correlations were made between slope in transition range and power in the inertial range: higher power leads to steeper spectrum

Bruno et al. ApJL **739** L14 (2014)

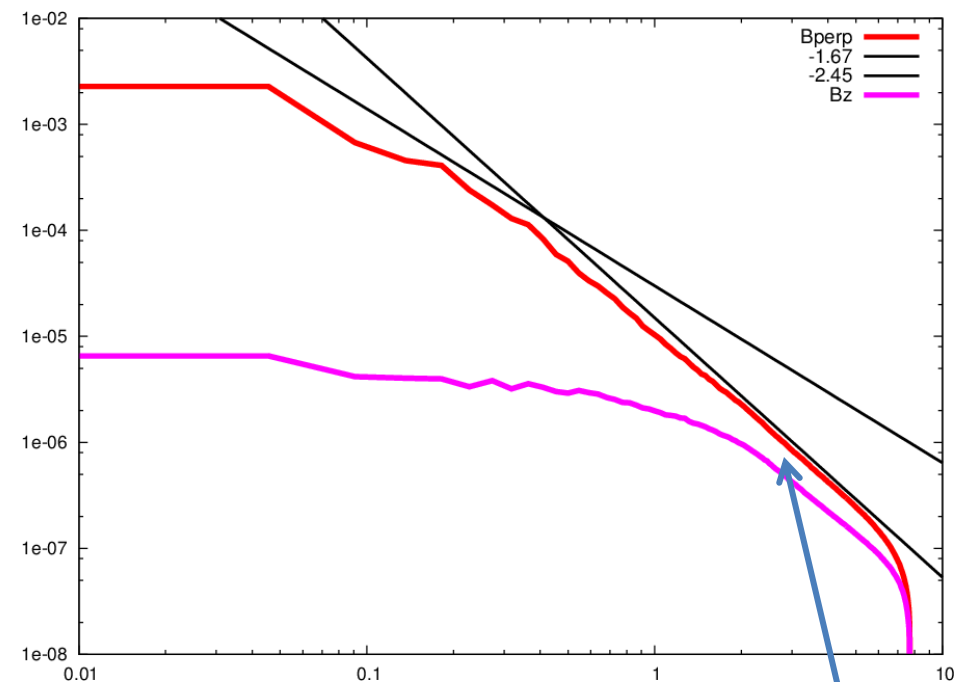
Present work

Two comments are in order:

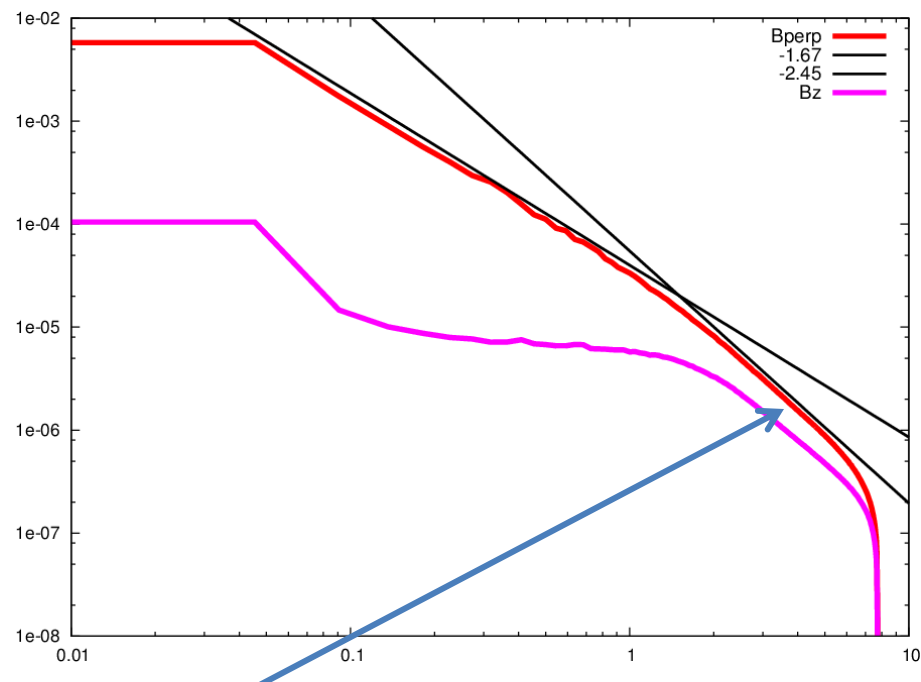
1. does not consider a transition range
2. the correlation is made with the nonlinearity parameter in the sub-ion range

When forcing is at a (larger) scale such that $k_{\perp}d_i=0.18/4$

$\delta B/B = 0.08$
Angle = 83.6°



$\delta B/B = 0.13$
Angle = 83.6°



Sub-ion slope very close in the two cases

Correlation of slopes vs. fluctuation amplitude depends at scale at which amplitude is measured. This is also seen in solar wind observations

Summary

Main features of the phenomenological model:

- Introduction of a new time scale associated with the homogenization process along magnetic field lines, induced by Landau damping
- The model predicts a **non-universal power-law spectrum** for strong turbulence at the **sub-ion scales** with an exponent which
 - depends on the saturation level of the nonlinearity parameter,
 - covers a range of values **consistent with solar wind and magnetosheath observations.**

3D FLR-Landau fluid simulations of Alfvénic turbulence at the ion scales

- Spectral index is **not universal** (varied by changing amplitude and angle of driven KAWs).
- Critical balance is satisfied when fluctuations are strong enough.
- Influence of Kolmogorov range on sub-ion range and of β still to be analyzed.

Conclusions

In situations where the distribution function is not too far from a Maxwellian, it is possible to recourse to fluid models to describe low frequency phenomena.

In order to address small-scale phenomena in directions quasi-perpendicular to the ambient magnetic field in plasmas with temperature anisotropy, fluid models should contain a minimum amount of complexity:

- equations for the fluid hierarchy up to heat fluxes
- finite Larmor radius corrections with the correct dependency on wave numbers (Bessel functions)
- closure that retains Landau damping for both ions and electrons.

The FLR-Landau fluid model can capture plasma heating, an issue of importance in accretion disks and in the intra-cluster medium, where the micro-instabilities have large-scale consequences.